Seasonal cycles and trends of water budget components in 18 river basins across the Tibetan Plateau: a multiple datasets perspective

Wenbin Liu[a], Fubao Sun[a*], Yanzhong Li[a], Guoqing Zhang[b,c], Yan-Fang Sang[a], Jiahong Liu[d], Hong Wang[a] ,Peng Bai[a]

[a]Key Laboratory of Water Cycle and Related Land Surface Processes, Institute of Geographic Sciences and Natural Resources Research, Chinese Academy of Sciences, Beijing 100101, China
[b]Key Laboratory of Tibetan Environmental Changes and Land Surface Processes, Institute of Tibetan Plateau Research, Chinese Academy of Sciences, Beijing 100101, China
[c]CAS Center for Excellent in Tibetan Plateau Earth Sciences, Beijing 100101, China
[d]Key Laboratory of Simulation and Regulation of Water Cycle in River Basin, China Institute of Water Resources and Hydropower Research, Beijing 100038, China

Submitted to: Hydrology and Earth System Sciences

Corresponding Author: Dr. Fubao Sun (Sunfb@igsnrr.ac.cn), from the Key Laboratory of Water Cycle and Related Land Surface Processes, Institute of Geographic Sciences and Natural Resources Research, Chinese Academy of Sciences (No. A11, Datun Road, Chaoyang District, Beijing 100101, China)

Email Addresses for other authors: Wenbin Liu (liuwb@igsnrr.ac.cn), Yanzhong Li (liyz.14b@igsnrr.ac.cn), Guoqing Zhang (guoqing.zhang@itpcas.ac.cn), Yan-fang Sang (sangyf@igsnrr.ac.cn), Jiahong Liu (liujh@iwhr.com) , Hong Wang (wanghong@igsnrr.ac.cn) , Peng Bai (baip.11b@igsnrr.ac.cn)

2016/11/25

Highlights

- Monthly basin-wide ET was calculated through water balance considering the impacts of glacier and water storage change
- Water budget components and trends for 18 river basins over the TP were evaluated
- Uncertainties were discussed from multiple dataset perspective

Abstract. The ~~insights~~ dynamics of water budget over the Tibetan Plateau (TP) are not fully understood so far due to the lack of quantitative observations of the land surface ~~processes~~water cycle. Here, we investigated the seasonal cycles and trends of water budget components, e.g., precipitation, runoff and evapotranspiration (ET), in 18 TP basins ~~through the use of~~using multi-source datasets during the period 1982-2011. A two-step bias correction procedure was applied to calculate the basin-wide ~~evapotranspiration (~~ET~~)~~ ~~through the water balance~~ considering the influences of glacier and water storage change. The results indicated that precipitation, which mainly concentrated during June-October (varied among different monsoons impacted basins), is the major contributor to the runoff in the TP basins. The basin-wide snow water equivalent (SWE) was relatively higher from mid-autumn to spring for most TP basins. The water cycles intensified under a global warming in most basins except for the upper Yellow and Yalong Rivers, which were significantly influenced by the weakening East Asian monsoon. ~~Corresponded to~~Consistent with the climate warming and moistening in the TP and western China, the aridity index (PET/P) in most basins decreased. ~~The general hydrological regimes could be inferred from the perspective of multi-source datasets although there are considerable uncertainties from different datasets, which are comparable to some existing studies using the field observations and complex modeling approaches.~~ The results highlighted the usefulness of integrating the multi-source data (e.g., in situ observations, remote sensing products, reanalysis, land surface model simulations and climate model outputs) for hydrological applications in the data-sparse ~~environments~~

regions and could be ~~benefit~~ beneficial for understanding the water and energy budgets, sustainable management of water resources under a warming climate in the harsh and the data-sparse Tibetan Plateau.

1 Introduction

As the highest plateau in the globe (the average elevation is higher than 4000 meters above the sea level), the Tibetan Plateau (TP, also called "the roof of the world" or "the third Pole") is one of the most vulnerable region under a warming climate and is subjected to strong interactions among atmosphere, hydrosphere, biosphere and cryosphere in the earth system (Duan and Wu, 2006; Yao et al., 2012; Liu W. et al., 2016b). It also serves as the "Asian water tower" ~~with~~ from which many major Asian rivers such as Yellow river, Yangtze river, Brahmaputra river, Mekong river, Indus river, etc., originate ~~from., which~~ It provides a vital water resource to support hundreds of millions of people in China and the surrounding countries (Immerzell et al., 2010; Zhang et al., 2013). Knowledge about the water budgets and their responses to the changing environment is thus crucial for understanding the hydrological regimes and for sustainable water resources management as well as environmental protection in this special region (Yang et al., 2014; Chen et al., 2015).

The TP is also known as a typical data-sparse mountain region which brings great challenges to hydrological and related land surface studies (Zhang et al., 2007; Li F. et al., 2013; Liu X. et al., 2016). For example, since the 1950s, totally 750 stations have been established over China by the Chinese Meteorological Administration (CMA), among which only less than 80 stations are distributed over the plateau (Wang and Zeng, 2012). They are primary sparse and unevenly located at relatively low elevation

regions, focus only on the meteorological variables and lack of other land surface observations such as evapotranspiration, snow water equivalent and latent heat fluxes, etc.. In addition, long-term consecutive observations of river discharge, snow depth, lake depth and glacier melts in the TP are also absent (Akhta et al., 2009; Ma et al., 2016). Therefore, the insights of water balance over various TP river basins ~~locates~~ located at different monsoon-dominant regions are~~, to some extent,~~ still unclear so far ~~due to the lack of quantitative observations of the land surface processes~~ (Cuo et al., 2014; Xu et al., 2016). One way to ~~break~~ overcome this limitation is to install more instruments to measure the ~~point scale~~in situ water budgets (Yang et al., 2013; Zhou et al., 2013; Ma et al., 2015), but it is extremely expensive to maintain long-term observations at ~~the harsh environment and is often difficult to be applied to~~ basin or regional scales. Another ~~more popular way~~workaround is to simulate basin-wide water budgets through physical-based land surface models at several large river basins forced with remote sensing data and large-scale gridded meteorological forcing datasets (Bookhagen and Burbank, 2010; Xue et al., 2013; Zhang et al., 2013; Cuo et al., 2015; Zhou et al., 2015; Wang et al., 2016). However, it is still difficult to use land surface models to multiple basins especially to the relatively smaller ones under complex terrains due to the lack of adequate data for model calibration and validation (Li F. et al., 2014).

~~it is also limited by the lack of adequate data for model calibration/validation and is hard to be used to multiple basins especially to relatively smaller basins under the complex terrains (Li F. et al., 2014).~~

~~In recent years, a~~A number of global (or regional) datasets for water budget components have been released recently including remote sensing-based retrievals

(Tapley et al., 2004; Zhang et al., 2010; Long et al., 2014; Zhang Y. et al., 2016), land surface model (LSM) simulations (Rui, 2011), reanalysis outputs (Berrisford et al., 2011; Kobayashi et al., 2015) and gridded forcing data interpolated from the in situ observations (Harries et al., 2014). For example, there are ~~considerable~~ many products for terrestrial evapotranspiration (ET) such as GLEAM_E (Global Land surface Evaporation: the Amsterdam Methodology, Miralles et al., 2011a), MTE_E (a product integrated the point-wise ET observation at FLUXNET sites with geospatial information extracted from surface meteorological observations and remote sensing in a machine-leaning algorithm, Jung et al., 2010), LSM-simulated ETs from Global Land Data Assimilation System version 2 (GLDAS-2) with different land surface schemes (Rodell et al., 2004), ETs from Japanese 55-year reanalysis (JRA55_E), the ERA-Interim global atmospheric reanalysis dataset (ERAI_E) and the National Aeronautic and Space Administration (NASA) Modern Era Retrosphective-analysis for Research and Application (MERRA) reanalysis data (Lucchesi, 2012). Moreover, there are also several global or regional LSM-based runoff simulations from GLDAS and the Variable Infiltration Capacity (VIC) model (Zhang et al., 2014). A few attempts have been made to validate multiple datasets for certain water budget components and to explore their possible hydrological implications, for example, Li X. et al. (2014) and Liu W. et al. (2016a) evaluated multiple ET estimates against the water balance method at annual and monthly time scales. Bai et al. (2016) assessed streamflow simulations of GLDAS LSMs in five major rivers over the TP based on the discharge observations. Although there are certain uncertainties among different datasets with various spatial and temporal resolutions and calculated through different algorithms (Xia et al., 2012), they do provide a great chance for us to quantify the general basin-wide water budgets and their uncertainties in gauge-sparse regions such

as the TP considered in this study.

The objectives of this study are (1) to investigate the general water budgets in 18 river basins across the Tibetan Plateau from the perspective of multiple datasets, and (2) to evaluate the seasonal cycles and annual trends of water budget components for 18 TP basins. The paper is organized as follows: the datasets and methods applied in this study are described in Sect.2. The results of season cycles and annual trends of water budget components for 18 TP basins are presented and discussed in Sect.3. The uncertainties inherited from multiple datasets are also discussed. In the Sect.4, we summarized the general results which would be helpful for understanding the water balances of the TP Rivers located at westerlies-dominated, Indian monsoon-dominated and East Asian monsoon-dominated regions.

2 Data and Method

2.1 Multiple datasets used

2.1.1 Study basins

Eighteen river basins over the TP (Fig.1) with the drainage area ranging from 2832 to 191235 km^2 (Table 1) are chosen in this study due to the availability of runoff data during the period 1982-2011. They mainly locate at the northwestern, southeastern and eastern parts of the plateau with multiyear-mean and basin-averaged temperature and precipitation ranging from -5.68 to 0.97 ^oC and 128 to 717 mm, which are solely or combined controlled by the westerlies, the Indian Summer monsoon and the Easter Asian monsoon (Yao et al., 2012). ~~The altitudes of the lowest and highest hydrological gauging stations are 1650 m and 4982 m above the sea level.~~ The glacier and snow covers are relatively more for the westerlies-dominant basins such as

158 Yerqiang, Yulongkashi and Keliya (10.86~23.27% and 29.16~35.95%, respectively)
159 whereas are less for the East Asian monsoon-dominated basins such as Yellow,
160 Yangtze and Bayin (0~0.96% and 9.42~20.05%, respectively) (Table 1).
161 <Figure 1, here please, thanks>
162 <Table 1, here please, thanks>
163 **2.1.2 Runoff, Precipitation and Terrestrial storage change**
164 Observed daily runoff (Q) during the period 1982-2011 ~~used for water balance~~
165 ~~calculation for 18 TP basins~~ was obtained from the National Hydrology Almanac of
166 China (Table 2). There are < 30% missing data in some gauging stations such as
167 Yajiang, Tongren, Gandatan and Zelingou. Therefore, the VIC Retrospective Land
168 Surface Dataset over China (1952~2012, VIC_IGSNRR simulated) with a spatial
169 resolution of 0.25 degree and a daily temporal resolution from the Geographic
170 Sciences and Natural Resources Research (IGSNRR), Chinese Academy of Sciences,
171 is also used. This dataset~~, which~~ is derived from the VIC model forced by the gridded
172 daily observed forcing (IGSNRR_forcing) (Zhang et al., 2014). A degree-day scheme
173 was used in the model to consider the influences of snow and glacier on hydrological
174 processes. ~~In this study, we first assess the VIC_IGSNRR-simulated runoff against the~~
175 ~~observations for each basin (for example, at Tangnaihai and Pangduo stations in~~
176 ~~Fig.2). The VIC_IGSNRR-simulated runoff is acceptable and could be used to replace~~
177 ~~the missing values for a given basin, if the Nash Efficiency coefficient (NSE) between~~
178 ~~the observation and simulation is above 0.65.~~
179 ~~< Figure 2, here please, thanks>~~
180
181 Monthly gridded precipitation dataset (0.5 degree, 1961-2011) form CMA, which was
182 interpolated from observations of 2472 national meteorological stations using the

Thin Plate Spline method, was used in this study (Table 2). Considering the uncertainty of CMA precipitation over the TP due to the relatively sparse stations ~~used~~ and the complex terrain conditions, two other precipitation datasets (IGSNRR_forcing and TRMM (Tropical Rainfall Measuring Mission) 3B43 V7, Huffman et al., 2012) were also ~~applied~~used. The precipitation from IGSNRR forcing datasets (0.25 degree) was derived by interpolating gauged daily precipitation from 756 CMA stations based on the synergraphic mapping system algorithm (Shepard, 1984; Zhang et al., 2014) and was further bias-corrected using the CMA gridded precipitation. ~~The CMA precipitation is perfectly consistent with TRMM (Corr = 0.86, RMSE = 8.34 mm/month) and IGSNRR forcing (Corr = 0.94, RMSE = 7.15mm/month) precipitation for multiple basins (and also for the smallest basin above Tongren station, Fig.2), which reveals the applicably of CMA precipitation under the TP conditions.~~

<Table 2, here please, thanks>

Three latest global terrestrial water storage anomaly and water storage change (ΔS) datasets (available on the GRACE Tellus website: http://grace.jpl.nasa.gov/) retrieved from the Gravity Recovery and Climate Experiment (GRACE, Tapley et al., 2004; Landerer and Swenson, 2012; Long et al., 2014), which were processed separately at the Jet Propulsion Laboratory (JPL), the GeoForschungsZentrum (GFZ) and the Center for Space Research at the University of Texas (CSR), were used. The GRACE retrievals (2002-2013) from three processing centers were averaged and a glacier isostatic adjustment correction as well a destriping filter were applied to minimize the errors and uncertainties of extracted ΔS.

2.1.3 Temperature, potential evaporation and ET

The CMA monthly gridded temperature (0.5 degree) and potential evaporation (PET)

dataset (0.5 degree, Harris et al., 2013) from Climatic Research Unit (CRU) in the University of East Anglia were used in this study. Moreover, six published global/regional ET products (four diagnostic products and two LSMs simulations, Table 2), namely (1) GLEAM_E (Miralles et al., 2010, 2011), which estimated three sources of ET (transpiration, soil evaporation and interception) separately through bare soil, short vegetation and vegetation with a tall canopy through a set of algorithm (www.gleam.eu), (2) GNoah_E simulated by GLDAS-2 with the Catchment Noah scheme (http://disc.sci.gsfc.nasa.gove/hydrology/data-holdings) (Rodell et al., 2004), (3) Zhang_E (Zhang et al., 2010) estimated using the modified Penman-Monteith approach forced with MODIS data, satellite-based vegetation parameters and meteorological observations (http://www.ntsg.umt.edu/project/et), (4) MET_E (Jung et al., 2010) (https://www.bgc-jena.mpg.de/geodb/projects/Home.phs), (5) VIC_E (Zhang et al., 2014) from VIC_IGSNRR simulations (http://hydro.igsnrr.ac.cn/public/vic_outputs.html) and (6) PML_E (Zhang Y. et al., 2016) computed from global observation-driven Penman-Monteith-Leuning (PML) model (https://data.csiro.au/dap/landingpage?pid=csiro:17375&v=2&d=true).

2.1.4 Vegetation and snow/glacier parameters

~~Two vegetation parameter datasets, t~~The Normalized Difference Vegetation Index (NDVI) and the Leaf Area Index (LAI) were used to quantify the dynamics of vegetation for 18 TP basins (Table 2). The NDVI data was obtained from the Global Inventory Modeling and Mapping Studies (GIMMS) (Turker et al., 2005) (https://nex.nasa.gov/nex/projects/1349/wiki/general_data_description_and_access/)

while the LAI data was collected from the Global Land Surface Satellite (GLASS) products (http://www.glcf.umd.edu/data/lai/) (Liang and Xiao, 2012). Seasonal snow and glacier are widespread over the plateau which significantly influences the water and energy budgets in the TP, but their observations are difficult due to the harsh environment, especially at the basin scale. However, there are currently a few satellite-based or LSM-simulated products which could provide general information about the variations of snow and glacier. The daily cloud free snow composite product from MODIS Terra-Aqua and the Interactive Multisensor Snow and Ice Mapping System for the Tibetan Plateau was applied to quantify the snow cover changes for each basin (Zhang et al., 2012; Yu et al., 2015). The snow water equivalent (SWE) retrieved from Global Snow Monitoring for Climate Research product (GlobSnow-2, http://www.globsnow.info/) and the VIC_IGSNRR simulations were also used in this study (Takala et al., 2011; Zhang et al., 2014). Moreover, the Second Glacier Inventory Dataset of China was used to extract the general distribution of glacier (Guo et al., 2014). All gridded datasets used were first uniformly interpolated to a spatial resolution of 0.5 degree based on the bilinear interpolation to make their inter-comparison possible. The datasets were then extracted for each of TP basins.

2.1.5 Monsoon indices

The TP climate is generally influenced by the westerlies, Indian summer monsoon and East Asian summer monsoon (Yao et al., 2012). To investigate the changes of monsoon systems and their potential influences on the water budget in the TP basins, three monsoon indices, namely Asian Zonal Circulation Index (AZCI), Indian Ocean Dipole Mode Index (IODMI) and East Asian Summer Monsoon Index (EASMI), are ~~also~~ used in this study. The IODMI is an indicator of the east-west temperature

gradient across the tropical Indian Ocean defined by Saji et al. (1999), which can be downloaded from the following website: http://www.jamstec.go.jp/frcgc/research/d1/iod/HTML/Dipole%20Mode%20Index.html. The EASMI and AZCI (60°-150°E) reflect the dynamics of East Asian summer monsoon (Li and Zeng, 2002) and the westerlies, which can be obtained from the http://ljp.gcess.cn/dct/page/65577 and the National Climate Center of China (http://ncc.cma.gov.cn/Website/index.php?ChannelID=43WCHID=5), respectively.

2.2 Methods

2.2.1 Water balance-based ET estimation

~~In this study, we first assess the VIC_IGSNRR simulated runoff against the observations for each basin (for example, at Tangnaihai and Pangduo stations in Fig.2). The VIC_IGSNRR simulated runoff is acceptable and could be used to replace the missing values for a given basin, if the Nash Efficiency coefficient (NSE) between the observation and simulation is above 0.65.~~

带格式的：居中

The basin-wide water balance at the monthly and annual timescales could ~~traditionally~~ be written as the principle of mass conservation (also known as the continuity equation, Oliverira et al., 2014) of basin-wide precipitation (P, mm), evapotranspiration (ET_{wb}, mm), runoff (Q, mm) as well as terrestrial water storage change (ΔS, mm),

$$ET_{wb} = P - Q - \Delta S \quad (1)$$

In most TP basins, glacier melt (M_G, mm) contributes to river discharge together with precipitation (liquid precipitation and snow). The monthly and annual water balance in these basins can thus be revised as,

$$ET_{wb} = P + M_G - Q - \Delta S \quad (2)$$

Several attempts have been made for separating glacier contributions to river discharge through site-scale isotopic observations, remote sensing as well as land-surface hydrological modeling for some individual TP basins (Zhang et al., 2013; Zhou et al., 2014; Neckel et al., 2014; Xiang et al., 2016). However, accurate quantification of M_G is difficult in the data-sparse TP, especially for multiple basins. In this study, we simply use the percentages of glacier melt to river discharge for some TP basins ~~concluded~~ derived from the ~~existing studies~~literatures (Chen, 1988; Mansur and Ajnis, 2005; Zhang et al., 2013; Liu J. et al., 2016) and the empirical relations between the glacier area ratio (%) and glacier melt in basins mentioned above (Table 3).

<Table 3, here please, thanks>

The terrestrial water storage (ΔS) in Eq.(2), which includes the surface, subsurface and ground water changes, cannot be neglected in water balance calculation at a monthly or annual timescale due to snow accumulation and some anthropogenic interferences such as reservoir regulation and agriculture irrigation (Liu W. et al., 2016a). The water balance-based ET (ET_{wb}) during 2002-2011 can be calculated through Eq. (2) using the GRACE-derived mass anomaly as ΔS. For ET_{wb} calculation before 2002 when the GRACE data is unavailable, we use a two-step bias correction procedure (Li X. et al., 2014) to close the water balance ~~for 18 basins~~ at monthly timescale considering the ΔS. We define $P + M_G - Q$ as biased ET (ET_{biased}, available from 1982-2011) relative to the ET_{wb} (available from 2002-2011 when the GRACE data is available) calculated from Eq. (2). Firstly, the ET_{biased} and ET_{wb} series over the period 2002-2011 were separately fitted using a gamma distribution, which has been evidenced as an proper method for modeling the probability distribution of ET (Bouraoui et al., 1999). The value in monthly ET_{biased}

306 series (2002-2011) can be bias-corrected through the inverse function (F^{-1}) of the
307 gamma cumulative distribution function (CDF, F) of ET_{wb} by matching the
308 cumulative probabilities between two CDFs as follow (Liu W. et al., 2016a),

309 $$ET_{wb}(m) = F^{-1}(F(ET_{biased}(m)|\alpha_{biased}, \beta_{biased})|\alpha_{wb}, \beta_{wb}) \quad (3)$$

310 Here $\alpha_{biased}, \beta_{biased}, \alpha_{wb}$ and β_{wb} are the shape and scale parameters of gamma
311 distribution for ET_{biased} and ET_{wb}. The second step is to eliminate the annual bias
312 through the ratio of annual ET_{biased} to annual ET_{wb} calculated in the first step using
313 the following method,

314 $$ET_{wb}(m) = \frac{ET_{biased}(a)}{ET_{wb}(a)} \times ET_{wb}(m) \quad (4)$$

315 The procedure was then applied to correct the monthly ET_{biased} series and calculated
316 the monthly ET_{wb} during the period 1982-2001 for all TP basins. The ET_{wb} obtained
317 was seemed as the "true" ET for evaluating multiple ET products and further for the
318 trend analysis.

319 **2.2.2 Modified Mann-Kendall test method**

320 The Mann-Kendall (MK) test is a rank-based nonparametric approach ~~and~~ which is
321 less sensitive to outlier relative to other parametric statistics~~. However, it is~~, but
322 ~~sometimes~~ it is sometimes ~~impacted~~ influenced by the serial correlation of time series.
323 Pre-whitening is often used to eliminate the influence of lag-1 autocorrelation before
324 the use of MK test, for example, in pre-whitening, the analyzed time series
325 $(X_1, X_2, \dots, X_n)$ will be replaced by $(X_2 - cX_1, X_3 - cX_2, \dots, X_{n+1} - cX_n)$ if the lag-1
326 autocorrelation coefficient (c) is larger than 0.1 (von Storch, 1995). However,
327 significant lag-i autocorrelation may still be detected after pre-whitening because only
328 the lag-1 autocorrelation is considered in pre-whitening (Zhang et al., 2013).
329 Moreover, it sometimes underestimate the trend for a given time series (Yue et al.,
330 2002). Hamed and Rao (1998) proposed a modified version of MK test (MMK) to

带格式的：字体：非倾斜

consider the lag-*i* autocorrelation and related robustness of the autocorrelation through the use of equivalent sample size, which has been widely used in previous studies during the last five decades (McVicar et al., 2012; Zhang et al., 2013; Liu and Sun, 2016).

In the MMK approach, if the lag-*i* autocorrelation coefficients are significantly distinct from zero, the original variance of MK statistics will be replaced by the modified one. ~~–~~In this study, we used ~~a modified version of MK test (MMK, Hamed and Rao, 1998)~~the MMK approach to quantify the trends of water budget components in18 TP basins~~.~~ and the significance of trend was tested at the >95% confidence level. ~~The MMK considers the lag-*i* autocorrelation and related robustness of the autocorrelation, which has been widely used in previous studies during the last five decades (McVicar et al., 2012; Liu and Sun, 2016).~~

带格式的：字体：非倾斜

带格式的：字体：非倾斜

3 Results and Discussion

3.1 ET evaluation and General hydrological characteristics of 18 TP basins

In this study, we first assess the VIC_IGSNRR simulated runoff against the observations for each basin (for example, at Tangnaihai and Pangduo stations in Fig.2). The VIC_IGSNRR simulated runoff is acceptable and could be used to replace the missing values for a given basin, if the Nash Efficiency coefficient (NSE) between the observation and simulation is above 0.65. Moreover, the CMA precipitation is consistent with TRMM (Corr = 0.86, RMSE = 8.34 mm/month) and IGSNRR forcing (Corr = 0.94, RMSE = 7.15mm/month) precipitation for multiple basins (and also for the smallest basin above Tongren station, Fig.2), which reveals the applicably of CMA precipitation under the TP conditions.

< Figure 2, here please, thanks>

We ~~first~~ then evaluated ~~monthly performances of~~ six ET products in 18 TP basins against ~~the~~our calculated ET_{wb} at a monthly basis~~, which was calculated through water balance considering the impacts of glacier and water storage change~~ (Fig. 3). The ranges of monthly averaged ET among different basins (approximately 4−39 mm $month^{-1}$) are very close for all products compare with that calculated from the ET_{wb}(6−42 mm $month^{-1}$). However, GLEAM_E (correlation coefficient: Corr = 0.85 and root-mean-square-error: RMSE = 5.69 mm $month^{-1}$) and VIC_E (Corr = 0.82 and RMSE = 6.16 mm $month^{-1}$) perform relatively better than others. Although Zhang_E and GNoah_E were found closely correlated to monthly ET_{wb} in the upper Yellow River, the upper Yangtze River, Qiangtang and Qaidam basins (Li X. et al., 2014), they did not exhibit overall good performances (Corr = 0.61, RMSE = 7.97 mm $month^{-1}$ for Zhang_E and Corr = 0.42, RMSE = 10.16 mm $month^{-1}$ for GNoah_E) for 18 TP basin used in this study. We thus use GLEAM_E and VIC_E together with ET_{wb} to calculate the seasonal cycles and trends of ET in 18 TP basins in the following sections.

< Figure 3, here please, thanks>

To investigate the general hydroclimatic characteristics of rivers over the TP, we classify 18 basins into three categories, namely westerlies-dominated basins (Yerqiang, Yulongkashi and Kelia), Indian monsoon-dominated basins (Brahmaputra and Salween), and East Asian monsoon-dominated basins (Yellow, Yalong and Yangtze) referred to Tian et al. (2007) ~~and ,~~ Yao et al. (2012~~, 2013~~) and Dong et al. (2016). Interestingly, they are clustered into three groups under ~~the perspective of~~ Budyko framework (Budyko, 1974; Zhang D. et al., 2016) with relatively lower evaporative index for Indian monsoon-dominant basins and higher aridity index for westerlies-dominant basins, which reveal various long-term hydroclimatologic

conditions (Fig. 4). Overall, the annual mean air temperature increases (-5.68 ~0.97 ^{o}C) while multiyear mean glacier area (and thus the glacier melt normalized by precipitation) decreases (23.27 ~ 0%) gradually from the westerlies-dominant, Indian monsoon-dominant to East Asian monsoon-dominant basins. The vegetation status (NDVI range: 0.05~0.43; LAI range: 0.03~0.83) tends to be better and ET increases (and thus runoff coefficient gradually decreases) from cold to warm basins (Fig. 4 and Table 1). The R^2 between basin-averaged NDVI and ET is 0.76 which shows a clear vegetation control on ET in 18 TP basins. The result is in line with Shen et al. (2015), which indicated that the spatial pattern of ET trend was significantly and positively correlated with NDVI trend over the TP. It is a general picture of hydrological regime in high-altitude and cold regions (Zhang et al., 2013; Cuo et al., 2014), which could be interpreted from the perspective of multi-source datasets in the data-sparse TP.

带格式的：上标

< Figure 4, here please, thanks>

3.2 Seasonal cycles of basin-wide water budget components for the TP basins

The multi-year means of water budget components (i.e., P, Q, ET, snow cover and SWE) and vegetation parameters (i.e., NDVI and LAI) were calculated for each calendar month and for 18 TP river basins ~~over~~ using multi-source datasets available from 1982 to 2011. Overall, the seasonal variations of P, Q, ET, air temperature and vegetation parameters are similar in all TP basins with peak values occurred in May to September (Fig.5 and Fig.6). The seasonal cycles of snow cover and SWE are generally time consistent as well for 18 TP basins (the peak values mainly occur from October to next April, Fig.7). With the ascending air temperature from cold to warm months, the basin-wide precipitation increases and vegetation turns green gradually (the basin-wide ET also increase). Meanwhile, glacier and snow melt or vanish gradually with the melt water supply the river discharge together with precipitation.

406 The inter-basin variations of hydrological regime are to a large extent linked to the
407 climate systems that prevail over the TP.
408 < Figure 5, here please, thanks>
409 Although the temporal patterns of hydrological components are general analogous,
410 they varied among parameters, climate zones and even basins (Zhou et al., 2005). For
411 example, relative to air temperature, the seasonal variation of runoff is more similar to
412 precipitation which reveals that runoff is mainly controlled by precipitation in ~~the~~
413 most TP basins. It is in agreement with that summarized by Cuo et al. (2014). In the
414 westerlies-dominated basins, the peak values of precipitation and runoff mainly
415 concentrate in June-August, which contribute approximately 68-82% and 67-78% of
416 annual totals, respectively. During this period, the runoff always exceeds precipitation
417 which indicates large contributions of glacier/snow-melt water to streamflow. It is
418 consistent with the existing findings in Tarim River (Yerqiang, Yulongkashi and
419 Keliya rivers are the major tributaries of Tarim River), which indicated that the melt
420 water accounted for about half of the annual total streamflow (Fu et al., 2008). The
421 ET (vegetation cover) in three westerlies-dominated basins are relatively less (scarcer)
422 than that in other TP basins while the percentages of glacier and seasonal snow cover
423 are higher in these basins which contribute more melt water to river discharge (Fig.6
424 and Fig.7). Overall, the SWE in Yerqiang, Yulongkashi and Keliya rivers are
425 relatively higher in winter than other seasons, but they vary with basins and products
426 which reveal considerable uncertainties in SWE estimations.
427 < Figure 6, here please, thanks>
428 In the Indian monsoon and East Asian monsoon-dominated basins, the runoff
429 concentrates during June-September (-or June- ~~June~~ October) with precipitation being
430 the dominant contributor of annual total runoff. For example, the peak values of

precipitation and runoff occur during June-September at Zhimenda station (contributing about 80% and 74% of the annual totals) while those occur during June-October at Tangnaihai station (contributing about 78% and 71% of the annual totals, respectively). The results are quite similar to the related studies in eastern and southern TP such as Liu (1999), Dong et al. (2007), Zhu et al. (2011), Zhang et al. (2013), Cuo et al. (2014). The vegetation cover (ET) in most basins is relatively better (higher) than that in the westerlies-dominant basins. Moreover, the seasonal snow mainly covers from mid-autumn to spring and correspondingly the SWE is relatively higher in these months in all basins except for Yellow River above Xining station, Salwee River above Jiayuqiao station and Brahmaputra River above Nuxia and Yangcun stations.

< Figure 7, here please, thanks>

3.3 Trends of basin-wide water budget components for the TP basins

Trends in water budget components for 18 TP basins during the period 1982-2011 were also examined through the modified Mann-Kendall test (MMK) in this study. The hydrological cycles intensified in the westerlies-dominated basins with Q, P and ET_{wb} all ascended with regional warming (Fig.8), especially in the Keliya River basin (Numaitilangan station). The aridity index (PET/P), which is an indicator for the degree of dryness, slightly declined in all basins in northwestern TP. Although P and PET were found both increase since the 1980s~~The results were in line with the overall climate warming and moistening reported in northwest China~~ (Shi et al., 2003; Yao et al., 2014)~~, at which these basins located.~~, the declined PET/P is, to some extent, attributed to the ascending P exceed the increase in PET for these basins (except for the Yulongkashi basin). The climate moistening in the headwaters of these inland rivers would be beneficial to the water resources and oasis agro-ecosystems in the

middle and lower basins. –The increase in streamflow was also found in most tributaries of the Tarim River (Sun et al., 2006; Fu et al., 2010; Mamat et al., 2010). Moreover, the westerlies, revealed by the Asian Zonal Circulation Index (60^{o}-150^{o} E), slightly enhanced (linear trend: 0.21) over the period of 1982-2011 (Fig.9). More water vapor was transported and fell as precipitation or snow in northwestern TP (e.g., the eastern Pamir region) with the strengthening westerlies. Both SWE products (VIC_IGSNRR simulated and GlobaSnow-2 product) showed slightly increase for all basins~~The SWE showed increase for all basins and for both products (VIC_IGSNRR simulated and GlobaSnow-2 product)~~ with the incremental seasonal snow cover and advanced glaciers (Yao et al., 2012). More precipitation was transformed into snow or glacier and the runoff coefficient (Q/P) exhibited decrease although precipitation obviously increased (Fig.8). In addition, the transpiration in these basins may decrease with vegetation degradation revealed by the NDVI and LAI (Yin et al., 2016) but the atmospheric evaporative demand indicated by CRU PET increased (significantly increase in the Yulongkashi and Keliya rivers) during the period 1982-2011.

< Figure 8, here please, thanks>

< Figure 9, here please, thanks>

In the East Asian monsoon-dominated basins, there are two types of change for basin-wide water budget components. For example, P and Q slightly decreased in the upper Yellow River (Tangnihai, Huangheyan and Jimai stations) and Yalong River (Yajiang station) but increased in other basins (Zelingou, Gandatan, Xining, Tongren and Zhimenda stations) over the period of 1982-2011 (Fig.10). The decline in Q and P for the upper Yellow and Yalong Rivers (locate at the eastern Tibetan Plateau) were consistent with that found by Cuo et al. (2013, 2014) as well as Yang et al. (2014), and were in line with the weakening (linear slope: -0.01) of the East Asian Summer

Monsoon (Fig.9). The vegetation turned green while ET_{wb} and PET increased in all nine basins with the significantly ascending air temperature during the period 1982-2011. The aridity index (PET/P) was found decrease in all basins except for the upper Yellow River basin above Jimai station and the upper Yalong River basin above Yajiang station. Moreover, ~~the~~both the ~~–~~runoff coefficients and SWE ~~(SWE)~~ were decrease ~~(decrease~~ except for the Bayin River above Zelingou station and the upper Yellow River above Tongren station~~)~~ in the East Asian monsoon dominated basins.

< Figure 10, here please, thanks>

The hydrological cycles were also found intensified in the Indian monsoon-dominated basins such as Salween River and Brahmaputra River (Fig.11), which were in line with the strengthen (linear trend: 0.~~0006~~01) of the Indian Summer monsoon (revealed by the Indian Ocean Dipole Mode Index) during the specific period 1982-2011 (Fig.9). In the six basins, trends in P, Q and ET_{wb} were all upward. For example, at Jiayuqiao station, the annual streamflow showed slightly increasing trend which was consistent with that examined during 1980-2000 by Yao et al. (2012). The vegetation status, revealed by NDVI and LAI, turned better significantly with the ascending air temperature. The aridity index (PET/P) decreased in all basins except for the Brahmaputra River above Tangjia station, which indicated that most basins in the Indian monsoon-dominated regions turn wet over the period of 1982-2011. The runoff coefficient (Q/P) increased at Gongbujiangda and Nuxia while decreased at Jiayuqiao, Pangduo, Tangji and Yangcun stations. Moreover, the basin-wide SWE declined in the upper Salween River and Brahmaputra River above Pangduo, Tangjia and Gongbujiangda stations while increased in Brahmaputra River above Nuxia and Yangcun stations.

< Figure 11, here please, thanks>

3.4 Uncertainties

The results may unavoidably associate with several aspects of uncertainties which mainly inherited from the multi-source datasets used. For example, although the seasonal cycles of ET_{wb} can be captured by GLEAM_E and VIC_E, they still have considerable uncertainties such as at Numaitilangan, Gongbujiangda and Nuxia stations (Fig.5). With respect to the annual trend of ET_{wb} (Table 4), most ET products (including the well-performed GLEAM_E and VIC_E in some basins) cannot detect the decreasing trends in 7 out of 18 basins (at Kulukelangan, Tongguziluoke, Xining, Tongren, Jimai, Nuxia and Gongbujiangda stations). We thus only used ET_{wb} in the trend detection of water budget components in Fig.8, Fig.10 and Fig.11 in this study. The two SWE products also showed large uncertainty, with respect to both their seasonal cycles and trends due to their different forcing data; different algorithms applied as well as varied spatial-temporal resolutions. Moreover, the interpolation of missing values of runoff with VIC_IGSNRR simulated runoff and the gridded precipitation data (which interpolated from limited gauged precipitation over the plateau) involved some uncertainties as well as. Finally, we obtained the contributions of glacier-melt to discharge in some basins from the literatures and took them as fixed numbers. It may inherit considerable uncertainty from varied studies using different approaches such as glacier mass-balance observation, isotope observation and hydrological modeling, and the contribution rates would also change under a warming climate. However, accurate quantification of the contribution of glacier-melt to discharge is technically difficult nowadays, especially for the data-sparse basins. ~~However, w~~With these caveats, we can interpret the general hydrological regimes and their responses to the changing climate in the TP basins from solely the perspective of multi-source datasets, which are comparable to the existing studies based on the in

situ observations and complex hydrological modeling.

<Table 4, here please, thanks>

4 Summary

In this study, we investigated the seasonal cycles and trends of water budget components in 18 TP basins during the period 1982-2011, which is not well understood so far due to the lack of adequate observations in the harsh environment, through integrating the multi-source global/regional datasets such as gauge data, satellite remote sensing and land surface model simulations. By using a two-step bias correction procedure, annual basin-wide ET_{wb} was calculated through the water balance considering the impacts of glacier and water storage change. The GLEAM_E and VIC_E were found perform better relative to other products against the calculated ET_{wb}.

The general water and energy budgets were different in the westerlies-dominated (with higher aridity index, runoff coefficient and glacier cover), the Indian monsoon-dominated and the East Asian monsoon-dominated (with higher air temperature, vegetation cover and evapotranspiration) basins under the perspective of Budyko framework. In 18 TP basins, precipitation is the major contributor to the river runoff, which concentrates mainly during June-October (June-August for the westerlies-dominated basins, June-September or June to October for the Indian monsoon-dominated and the East Asian monsoon-dominated basins). The basin-wide SWE is relatively higher from mid-autumn to spring for all 18 TP basins except for Keliya River and Brahmaputra River above the Nuxia and Yangcun stations. The vegetation cover is relatively less whereas snow/glacier cover is more in the westerlies-dominant basins compared with other basins. The hydrological cycles were

found intensified under the regional warming in most TP basins except for most tributaries of the upper Yellow River and the Yalong River, which were significantly influenced by the weakening East Asian monsoon during the period 1982-2011. The aridity index (PET/P) exhibited decrease in most TP basins which corresponded to the warming and moistening climate in the TP and western China. Moreover, the runoff coefficient (Q/P) declined in most basins which may be, to some extent, due to ET increase induced by vegetation greening and the influences of snow and glacier changes. Although there are considerable uncertainties inherited from multi-source data used, the general hydrological regimes in the TP basins could be revealed, which are consistent to the existing results obtained from in situ observations and complex land surface modeling. It indicated the usefulness of integrating the multiple datasets available such as in situ observations, remote sensing-based products, reanalysis outputs, land surface model simulations and climate model outputs for hydrological applications. The results obtained could be helpful for understanding the hydrological ~~cycles,~~cycles and further for the water resources management and eco-environment protection under a warming climate in the vulnerable Tibetan Plateau.

Author contributions. Wenbin Liu and Fubao Sun developed the idea to see the general water budgets in the TP basins from the perspective of multisource datasets. Wenbin Liu collected and processed the multiple datasets with the help of Yanzhong Li, Guoqing Zhang, Hong Wang as well as Peng Bai, and prepared the manuscript. The results were extensively commented and discussed by Fubao Sun, Jiahong Liu and Yan-Fang Sang.

Acknowledgements. This study was supported by the National Key Research and Development Program of China (2016YFC0401401 and 2016YFA0602402),National

Natural Science Foundation of China (41401037 and 41330529), the Open Research Fund of State Key Laboratory of Desert and Oasis Ecology in Xinjiang Institute of Ecology and Geography, Chinese Academy of Sciences (CAS), the CAS Pioneer Hundred Talents Program (Fubao Sun), the Initial Founding of Scientific Research (Y5V50019YE) and the program for the "Bingwei" Excellent Talents from the Institute of Geographic Sciences and Natural Resources Research, CAS. We are grateful to the NASA MEaSUREs Program (Sean Swenson) for providing the GRACE land data processing algorithm. The basin-wide water budget series in the TP Rivers used in this study are available from the authors upon request (liuwb@igsnrr.ac.cn). We wish to thank the editors and reviewers for their invaluable comments and constructive suggestions to improve the quality of the manuscript.

References

Akhtar, M., Ahmad, N., and Booij, M.J.: Use of regional climate model simulations as input for hydrological models for the Hindukush-Karakorum-Himalaya region, Hydrol. Earth Syst. Sci. 13, 1075-1089, 2009.

Bai, P., Liu, X.M., Yang, T.T., Liang, K., and Liu, C.M.: Evaluation of streamflow simulation results of land surface models in GLDAS on the Tibetan Plateau, J. Geophys. Res. Atmos., 121, 12180-12197, 2016.

Berrisford, P, Lee, D., Poli, P., Brugge, R., Fielding, K., Fuentes, M., Kallberg, P.,Kobayashi, S., Uppala, S., and Simmons, A.: The ERA-interim archive. ERA Reports Series No. 1 Version 2.0, Available from: <https://www.researchgate.net/publication/41571692_The_ERA-interim_archive>, 2011.

Bookhagen, B. and Burbank, D.W.: Toward a complete Himalayan hydrological budget: spatiotemporal distribution of snowmelt and rainfall and their impact on river discharge, J. Geophys. Res., 115, F03019, 2010.

Bouraoui, F., Vachaud, G., Li, L.Z.X., LeTreut, H., and Chen, T.: Evaluation of the impact of

609 climate changes on water storage and groundwater recharge at the watershed scale, Clim. Dyn.,
610 15(2), 153-161, 1999.
611 Budyko, M.I.: Climate and life. Academic Press, 1974.
612 Chen, D., Xu, B., Yao, T., Guo, Z., Cui, P., Chen, F., Zhang, R., Zhang, X., Zhang, Y., Fan, J., Hou,
613 Z., and Zhang, T.: Assessment of past, present and future environmental changes on the Tibetan
614 Plateau, Chinese SCI. Bull., 60(32), 3025-3035, 2015 (in Chinese).
615 Chen, J.: Lichenometrical studies on glacier changes during the Holocene Epoch at the sources
616 region of Urumqi River, Sci. China B., 18(1), 95-104, 1988 (in Chinese).
617 Cuo, L., Zhang, Y.X., Bohn, T.J., Zhao, L., Li, J.L., Liu, Q.M., and Zhou, B.R.: Frozen soil
618 degradation and its effects on surface hydrology in the northern Tibetan Plateau, J. Geophys.
619 Res. Atmos., 120(6), 8276-8298, 2015.
620 Cuo, L., Zhang, Y.X., Gao, Y., Hao, Z., and Cairang, L.: The impacts of climate change and land
621 cover/use transition on the hydrology in the upper Yellow River Basin, China, J. Hydrol., 502,
622 37-52, 2013.
623 Cuo, L., Zhang, Y.X., Zhu, F.X., and Liang, L.Q.: Characteristics and changes of streamflow on
624 the Tibetan Plateau: A review, J. Hydrol. Reg. stud., 2, 49-68, 2014.
625 Dong, X., Yao, Z., and Chen, C.: Runoff variation and responses to precipitation in the source
626 regions of the Yellow River, Resour. Sci., 29(3), 67-73, 2007 (in Chinese).
627 Dong, W., Lin, Y., Wright, J.S., Ming, Y., Xie, Y., Wang, B., Luo, Y., Huang, W., Huang, J., Wang,
628 L., Tian, L., Peng, Y., and Xu, F.: Summer rainfall over the southwestern Tibetan Plateau
629 controlled by deep convection over the Indian Subcontinent, Nat. Commun., 7, 10925, 2016.
630 Duan, A.M. and Wu, G.X.: Change of cloud amount and the climate warming on the Tibetan
631 Plateau, Geophys. Res. Lett., 33, L22704, 2006.
632 Fu, L., Chen, Y., Li, W., Xu, C., and He, B.: Influence of climate change on runoff and water
633 resources in the headwaters of the Tarim River, Arid Land Geogr., 31(2), 237-242, 2008 (in
634 Chinese).
635 Fu, L., Chen, Y., Li, W., He, B., and Xu, C.: Relation between climate change and runoff volume
636 in the headwaters of the Tarim River during the last 50 years., J. Desert Res., 30(1), 204-209,
637 2010 (in Chinese).
638 Guo, W.Q., Liu, S.Y., Yao, X.J., Xu, J.L., Shangguan, D.H., Wu, L.Z., Zhao, J.D., Liu, Q., Jiang,

639 Z.L., Wei, J.F., Bao, E.J., Yu, P.C., Ding, L.F., Li, G., Ge, C.M., and Wang, Y.: The Second
640 Glacier Inventory Dataset of China, Cold and Arid Regions Science Data Center at Lanzhou,
641 doi: 10.3972/glacier.001.2013.db, 2014.
642 Hamed, K.H. and Rao, A.R.: A modified Mann-Kendall trend test for autocorrelation data,
643 J.Hydrol., 204(1-4), 182-196, 1998.
644 Huffman, G.J., , E.F., Bolvin, D.T., Nelkin, E.J., and Adler, R.F.: last updated 2013: TRMM
645 Version 7 3B42 and 3B43 Data Sets, NASA/GSFC, Greenbelt, MD. Data set accessed at
646 http://mirador.gsfc.nasa.gov/cgibin/mirador/
647 presentNavigation.pl?tree=project&project=TRMM&dataGroup=Gridded&CGIS
648 ESSID=5d12e2ffa38ca2aac6262202a79d882a, 2012.
649 Harris, I., Jones, P.D., Osborn, T.J., and Lister, D.H.: Updated high-resolution grids of monthly
650 climatic observations – the CRU TS3.10 Dataset, Int. J. Climatol., 34 (3), 623-642, 2014.
651 Immerzeel, W.W., van Beek, L.P.H., and Bierkens, M.F.P.: Climate change will affect the Asian
652 water towers, Science, 328, 1382-1385, 2010.
653 Jung, M., Reichstein, M., Ciais, P., Seneviratne, S.I., Sheffield, J., Goulden, M.L., Bonan, G.,
654 Cescatti, A., Chen, J., de Jeu, R., Dolman, A.J., Eugster, W., Gerten, D., Gianelle, D., Gobron, N.,
655 Heinke, J., Kimball, J., Law, B.E., Montagnani, L., Mu, Q., Mueller, B., Oleson, K., Papale, D.,
656 Richardson, A.D., Roupsard, O., Running, S., Tomelleri, E., Viovy, N., Weber, U., Williams, C.,
657 Wood, E., Zaehle, S., and Zhang, K.: Recent decline in the global land evapotranspiration trend
658 due to limited moisture supply, Nature, 467, 951-954, 2010.
659 Kobayashi, S., Ota, Y., Harada, Y., Ebita, A., Moriya, M., Onoda, H., Onogi, K., kamahori, H.,
660 kobayashi, C., Endo, H., miyaoka, K., and Takahashi, K.: The JRA-55 Reanalysis: General
661 specifications and basic characteristics, J.Meteor. Soc. Japan, 93(1), 5-58, doi:
662 10.2151/jmsj.2015-001, 2015.
663 Landerer, F.W. and Swenson, S.C.: Accuracy of scaled GRACE terrestrial water storage estimates,
664 Water Resour.Res., 48, W04531, 2012.
665 Li, F.P., Zhang, Y.Q., Xu, Z.X., Liu, C.M., Zhou, Y.C., and Liu, W.F.: Runoff predictions in
666 ungauged catchments in southeast Tibetan Plateau, J. Hydrol., 511, 28-38, 2014.

667 Li, F.P., Zhang, Y.Q., Xu, Z.X., Teng, J., Liu, C.M., Liu, W.F., and Mpelasoka, F.: The impact of
668 climate change on runoff in the southeastern Tibetan Plateau, J. Hydrol., 505, 188-201, 2013.
669 Li, J.P. and Zeng, Q.C.: A unified monsoon index, Geophy. Res. Lett., 29(8), 1274, 2002.
670 Li, X.P., Wang, L., Chen, D.L., Yang, K., and Wang, A.H.: Seasonal evapotranspiration changes
671 (1983-2006) of four large basins on the Tibetan Plateau, J. Geophys. Res., 119 (23),
672 13079-13095, 2014.
673 Liang, S.L.and Xiao, Z.Q.: Global Land Surface Products: Leaf Area Index Product Data
674 Collection(1985-2010), Beijing Normal University, doi:10.6050/glass863.3004.db, 2012.
675 Liu, J., Liu, T., Bao, A., De Maeyer, P., Feng, X., Miller, S.N., and Chen, X.: Assessment of
676 different modeling studies on the spatial hydrological processes in an arid alpine catchment,
677 Water Resour. Manag., 30, 1757-1770, 2016.
678 Liu, T.: Hydrological characteristics of Yalungzangbo River, Acta Geogr. Sin., 54 (Suppl.),
679 157-164, 1999 (in Chinese).
680 Liu, W.B. and Sun, F.B.: Assessing estimates of evaporative demand in climate models using
681 observed pan evaporation over China, J. Geophys. Res. Atmos., 121, 8329-8349, 2016.
682 Liu, W.B., Wang, L., Zhou, J., Li, Y.Z., Sun, F.B., Fu, G.B., Li, X.P., and Sang, Y-F.: A worldwide
683 evaluation of basin-scale evapotranspiration estimates against the water balance method, J.
684 Hydrol., 538, 82-95, 2016a.
685 Liu, W.B., Wang, L., Chen, D.L., Tu, K., Ruan, C.Q., and Hu, Z.Y.: Large-scale circulation
686 classification and its links to observed precipitation in the eastern and central Tibetan Plateau,
687 Clim. Dyn., 46, 3481-3497, 2016b.
688 Liu, X.M., Yang, T., Hsu, K., Liu, C., and Sorooshian, S.: Evaluating the streamflow simulation
689 capability of PERSIANN-CDR daily rainfall products in two river basins on the Tibetan Plateau,
690 Hydrol. Earth Syst. Sci. Discuss., doi: 10.5194/hess-20160282, 2016.
691 Long, D., shen, Y.J., Sun, A., Hong, Y., Longuevergne, L., Yang, Y.T., Li, B., and Chen, L.:
692 Drought and flood monitoring for a large karst plateau in Southwest China using extended
693 GRACE data, Remote Sen. Environ., 155, 145-160, 2014.

694 Lucchesi, R.: File specification for MERRA products, GMAO Office Note No.1 (version 2.3), 82
695 pp, available from http://gmao.gsfc.nasa.gov/pubs/office_notes, 2012.
696 Ma, N., Szilagyi, J., Niu, G.Y., Zhang, Y.S., Zhang, T., Wang, B.B., and Wu, Y.H.: Evaporation
697 variability of Nam Co Lake in the Tibetan Plateau and its role in recent rapid lake expansion, J.
698 Hydrol., 537, 27-35, 2016.
699 Ma, N., Zhang, Y.S., Guo, Y.H., Gao, H.F., Zhang, H.B., and Wang, Y.F.: Environmental and
700 biophysical controls on the evapotranspiration over the highest alpine steppe, J. Hydrol., 529,
701 980-992, 2015.
702 Mamat, A., Halik, W., and Yang, X.: The climatic changes of Qarqan river basin and its impact on
703 the runoff, Xinjiang Agric. Sci., 47 (5), 996-1001, 2010 (in Chinese).
704 Mansur, S. and Ajinisa, T.: An analysis of water resources and it's hydrological characteristics of
705 Yarkend River Valley, J. Xinjiang Norm. Univ. (Nat. Sci. Ed.), 24(1), 74-78, 2005 (in Chinese).
706 McVicar, T.R., Roderick, M., Donohue, R.J., Li, L.T., Van Niel, T.G., Thomas, A., Grieser, J.,
707 Jhajharia, D., Himri, Y., Mahowald, N.M., Mescherskaya, A.V., Kruger, A.C., Rehman, S., and
708 Dinpashoh, Y.: Global review and synthesis of trends in observed terrestrial near-surface wind
709 speeds: implications for evaporation, J. Hydrol., 416-417, 182-205, 2012.
710 Miralles, D.G., De Jeu, R.A.M., Gash, J.H., Holmes, T.R.H., and Dolman, A.J.: Magnitude and
711 variability of land evaporation and its components at the global scale, Hydrol. Earth Syst. Sci., 15,
712 967-981, 2011.
713 Miralles, D.G., Gash, J.H., Holmes, T.R.H., de Jeu, R.A.M, and Dolman, A.J.: Global canopy
714 interception from satellite observations, J. Geophys. Res., 115, D16122, 2010.
715 Neckel, N., Kropáček, J., Bolch, T., and Hochschild, V.: Glacier mass changes on the Tibetan
716 Plateau 2003-2009 derived from ICESat laser altimetry measurements, Environ. Res. Lett., 9,
717 014009(7pp), 2014.
718 Oliveira, P.T.S., Mearing, M.A., Moran, M.S., Goodrich, D.C., Wendland, E., and Gupta, H.V.:
719 Trends in water balance components across the Brazilian Cerrado, Water Resour. Res., 50,
720 7100-7114, 2014.
721 Rodell, M., Houser, P.R., Jambor, U., Gottschalck, J., Mitchell, K., Meng, C.-J., Arsenault, K.,
722 Cosgrove, B., Radakovich, J., Bosilovich, M., Entin, J.K., Walker, P., Lohmann, D., and Toll, D.:
723 The global land data assimilation system, B. Am. Meteorol. Soc., 85, 381-394, 2004.

724 Rui, H.: README Document for Global Land Data Assimilation System Version 2 (GLDAS-2)
725 Products, GES DISC, 2011.
726 Saji, N.H., Goswami, B.N., Vinayachandran, P.N., and Yamagata, T.: A dipole mode in the tropical
727 Indian Ocearn, Nature, 401, 360-363, 1999.
728 Shen, M.G., Piao, S.L., Jeong, S., Zhou, L.M., Zeng, Z.Z., Ciais, P., Chen, D.L., Huang, M.T., Jin,
729 C.S., Li, L.Z.X., Li, Y., Myneni, R.B., Yang, K., Zhang, G.X., Zhang, Y.J., and Yao, T.D.:
730 Evporative cooling over the Tibetan Plateau induced by vegetation growth, Proc. Natl. Acad.
731 Sci. U. S.A., 112(30), 9299-9304, 2015.
732 Shi, Y.F., Shen, Y.P., Li, D.L., Zhang, G.W., Ding, Y.J., Hu, R.J., and Kang, E.S.: Discussion on
733 the present climate change from Warm2dry to Warm2wet in northwest China, Quat. Sci., 23(2),
734 152-164, 2003 (in Chinese).
735 Shepard, D.S.: Computer mapping: the SYMAP interpolation algorithm. Spatial Statistics and
736 Models, G.L. Gaile and C.J. Willmott, Eds., D. Reidel, 133-145, 1984.
737 Sun, B., Mao, W., Feng, Y., Chang, T., Zhang, L., and Zhao, L.: Study on the change of air
738 temperature, precipitation and runoff volume in the Yarkant River basin, Arid Zone Res., 23(2),
739 203-209, 2006 (in Chinese).
740 Takala, M., Luojus, K., Pulliainen, J., Derksen, C., Lemmetyinen, J., Kärnä, J.-P, Koskinen, J., and
741 Bojkov, B.: Estimating northern hemisphere snow water equivalent for climate research through
742 assimilation of spaceborne radiometer data and ground-based measurements, Remote
743 Sens. .Environ., 115 (12), 3517-3529, 2011.
744 Tapley, B.D., Bettadpur, S., Watkins, M., and Rand eigber, C.: The gravity recovery and climate
745 experiment: mission overview and early results, Geophys. Res. Lett., 31, L09607, 2004.
746 Tian, L., Yao, T., MacClune, K., White, J.W.C.., Schilla, A., Vaughn, B., Vachon, R., and
747 Ichiyanagi, K.: Stable isotopic variations in west China: a consideration of moisture sources, J.
748 Geophys. Res. Atmos., 112, D10112, 2007.
749 Tucker, C.J., Pinzon, J.E., Brown, M.E., Slayback, D., Pak, E.W., Mahoney, R., Vermote, E., and
750 El Saleous, N.: An extended AVHRR 8 km NDVI data set compatible with MODIS and SPOT
751 vegetation NDVI data, Int. J. Remote Sens., 26(20), 4485-4498, 2005.

752 von Storch, H.: Misuses of statistical analysis in climate research, In Analysis of Climate
753 Variability: Applications of Statistical Techniques, Springer-Verlag: Berlin, 11-26, 1995.
754 Wang, A. and Zeng, X.:Evaluation of multireanalysis products within site observations over the
755 Tibetan Plateau, J. Geophys. Res., 117, D05102, 2012.
756 Wang, L., Sun, L.T., Shrestha, M., Li, X.P., Liu, W.B., Zhou, J., Yang, K., Lu, H., and Chen, D.L.:
757 Improving snow process modeling with satellite-based estimation of
758 near-surface-air-temperature lapse rate, J. Geophys. Res. Atmos., 121, 12005-12030, 2016.
759 Xia, Y., Mitchell, K., Ek, M., Cosgrove, B., Sheffield, J., Luo, L., Alonge, C., Wei, H., Meng, J.,
760 Livneh, B., and Duang, Q.: Continental-scale water and energy flux analysis and validation for
761 North American Land Data Assimilation System project phase 2 (NLDAS-2): 2. Validation of
762 model-simulated streamflow, J. Geophys. Res. Atmos., 117(D3), D03110, 2012.
763 Xiang, L., Wang, H., Steffen, H., Wu, P., Jia, L., Jiang, L., and Shen, Q.: Groundwater storage
764 changes in the Tibetan Plateau and adjacent areas revealed from GRACE satellite gravity data,
765 Earth Planet. Sci. Lett., 449, 228-239, 2016.
766 Xu, L.: The land surface water and energy budgets over the Tibetan Plateau, Available from
767 Nature Precedings < http://hdl.handle.net/10101/npre.2011.5587.1>, 2011.
768 Xue, B.L., Wang, L., Yang, K., Tian, L., Qin, J., Chen, Y., Zhao, L., Ma, Y., Koike, T., Hu, Z., and
769 Li, X.P.: Modeling the land surface water and energy cycle of a mesoscale watershed in the
770 central Tibetan Plateau with a distributed hydrological model, J. Geophys. Res. Atmos., 118,
771 8857-8868, 2013.
772 Yao, Z., Duan, R., and Liu, Z.: Changes in precipitation and air temperature and its impacts on
773 runoff in the Nujiang River basins. Resour. Sci. 34(2), 202-210, 2012 (in Chinese)
774 Yang, K., Qin, J., Zhao, L., Chen, Y.Y., Tang, W.J., Han, M.L., Lazhu, Chen, Z.Q., Lv, N., Ding,
775 B.H., Wu, H., and Lin, C.G.: A multi-scale soil moisture and freeze-thaw monitoring network
776 on the third pole, Bull. Am. Meteorol. Soc., 94,1907-1916, 2013.
777 Yang, K., Wu, H., Qin, J., Lin, C.G., Tang, W.J., and Chen, Y.Y.: Recent climate changes over the
778 Tibetan Plateau and their impacts on energy and water cycle: a review, Glob. Planet Change,
779 112, 79-91, 2014.
780 Yao, T.D., Thompson, L., Yang, W., Yu, W.S., Gao, Y., Guo, X.J., Yang, X.X., Duan, K.Q., Zhao,
781 H.B., Xu, B.Q., Pu, J.C., Lu, A.X., Xiang, Y., Kattel, D.B., and Joswiak, D.: Different glacier

782 status with atmospheric circulations in Tibetan Plateau and surroundings, Nat. Clim. Change, 2,
783 1-5, 2012.
784 Yao, Y.J., Zhao, S.H., Zhang, Y.H., Jia, K., and Liu, M.: Spatial and decadal variations in potential
785 evapotranspiration of China based on reanalysis datasets during 1982-2010, Atmosphere, 5,
786 737-754, 2014.
787 Yin, G., Hu, Z.Y., Chen, X., and Tiyip, T.: Vegetation dynamics and its response to climate change
788 in Central Asia, J. Arid Land, 8, 375, 2016.
789 Yu, J., Zhang, G., Yao, T., Xie, H., Zhang, H., Ke, C., and Yao, R.: Developing daily cloud-free
790 snow composite products from MODIS Terra-Aqua and IMS for the Tibetan Plateau, IEEE
791 Trans. Geosci. Remote Sens., 54(4), 2171-2180, 2015.
792 Yue, S., Pilon, P., Phinney, B., Cavadias, G.: The influence of autocorrelation on the ability to
793 detect trend in hydrological series, Hydrol. Process., 16(9), 1807-1829, 2002.
794 Zhang, D., Liu, X., Zhang, Q., Liang, K., and Liu, C.: Investigation of factors affecting
795 intea-annual variability of evapotranspiration and streamflow under different climate conditions.
796 J. Hydrol., doi:10.1016/j.jhydrol.2016.10.047, 2016.
797 Zhang, G., Xie, H., Yao, T., Liang, T., and Kang, S.: Snow cover dynamics of four lake basins
798 over Tibetan Plateau using time series MODIS data (2001-2100), Water Resour. Res., 48(10),
799 W10529, 2012.
800 Zhang, K., Kimball, J.S., Nemani, R.R., and Running, S.W.: A continuous satellite-derived global
801 record of land surface evapotranspiration from 1983 to 2006, Water Resour. Res., 46(9),
802 W09522, 2010.
803 Zhang, L., Su, F., Yang, D., Hao, Z., and Tong, K.: Discharge regime and simulation for the
804 upstream of major rivers over Tibetan Plateau, J. Geophys. Res. Atmos., 118(15), 8500-8518,
805 2013.
806 Zhang, Q., Li, J., Singh, V., and Xu, C.: Copula-based spatial-temporal patterns of precipitation
807 extremes in China, Int. J. Climatol., 33, 1140-1152, 2013.
808 Zhang, X., Tang, Q., Pan, M., and Tang, Y.: A long-term land surface hydrologic fluxes and states
809 dataset for China, J. Hydrometeorol., 15, 2067-2084, 2014.
810 Zhang, Y., Peña-Arancibia, J.L., McVicar, T.R., Chiew, F.H.S., Vaze, J., Liu, C.M., Lu, X.J.,
811 Zheng, H.X., Wang, Y.P., Liu, Y.Y., Miralles, D.G., and Pan, M.: Multi-decadal trends in global

812 terrestrial evapotranspiration and its components, Scientific Reports, 6, 19124, 2016.
813 Zhang, Y., Liu, C., Tang, Y., and Yang, Y.: Trend in pan evaporation and reference and actual
814 evapotranspiration across the Tibetan Plateau, J. Geophys. Res., 112, D12110, 2007.
815 Zhou, C., Jia, S., Yan, H., and Yang, G.: Changing trend of water resources in Qinghai Province
816 from 1956 to 2000, J. Glaciol. Geocryol., 27(3), 432-437, 2005 (in Chinese).
817 Zhou, J., Wang, L., Zhang, Y.S., Guo, Y.H., Li, X.P., and Liu, W.B.: Exploring the water storage
818 changes in the largest lake (Selin Co) over the Tibetan Plateau during 2003-2012 from a
819 basin-wide hydrological modeling,. Water Resour. Res., 51, 8060-8086, 2015.
820 Zhou, S.Q., Kang, S., Chen, F., and Joswiak, D.R.: Water balance observations reveal significant
821 subsurface water seepage from Lake Nam Co., south-central Tibetan Plateau,. J. Hydrol., 491,
822 89-99, 2013.
823 Zhou, S.Q., Wang, Z., and Joswiak, D.R.:From precipitation to runoff: stable isotopic fractionation
824 effect of glacier melting on a catchment scale, Hydrol. Process., 28(8), 3341-3349, 2014.
825 Zhu, Y., Chen, J., Chen, G.: Runoff variation and its impacting factors in the headwaters of the
826 Yangtze River in recent 32 years, J.Yangtze River Sci. Res. Inst., 28(6), 1-4, 2011 (in Chinese).

Table 1: Main features of the 18 used TP river basins. GA% and SC% represent the percentages of multiyear-mean glacier cover and snow cover in each basin. The glacier and snow cover data are extracted, respectively, from the Second Glacier Inventory Dataset of China and the daily TP snow cover dataset (2005-2013)

No.	Station	Altitude (m)	River name	Drainage area (km^2)	Multiyear-mean (1982-2011) and basin-averaged parameters						
					Q (mm/yr)	Prec. (mm/yr)	Temp.(^oC/yr)	NDVI	LAI	GA%	SC%
01	Kulukelangan	2000	Yerqiang	32880.00	158.60	128.34	-5.68	0.05	0.03	10.97	35.03
02	Tongguziluoke	1650	Yulongkashi	14575.00	151.56	134.04	-4.07	0.06	0.04	23.27	35.95
03	Numaitilangan	1880	Keliya	7358.00	103.18	137.14	-4.78	0.06	0.03	10.86	29.16
04	Zelingou	4282	Bayin	5544.00	41.42	340.68	-4.98	0.13	0.09	0.09	21.22
05	Gadatan	3823	Yellow	7893.00	200.95	566.01	-4.60	0.34	0.54	0.13	14.94
06	Xining	3225	Yellow	9022.00	99.90	503.74	0.97	0.36	0.70	0.00	10.06
07	Tongren	3697	Yellow	2832.00	149.36	533.25	-1.37	0.39	0.83	0.00	9.42
08	Tainaihai	2632	Yellow	121972.00	159.48	540.32	-2.40	0.34	0.72	0.09	15.89
09	Huangheyan	4491	Yellow	20930.00	31.18	386.42	-4.81	0.23	0.61	0.00	17.25
10	Jimai	4450	Yellow	45015.00	85.50	441.48	-4.16	0.26	0.52	0.00	20.05
11	Yajiang	2599	Yalong	67514.00	237.66	717.05	-0.23	0.43	0.80	0.15	18.36
12	Zhimenda	3540	Yangtze	137704.00	96.23	405.66	-4.83	0.20	0.26	0.96	17.87
13	Jiaoyuqiao	3000	Salween	72844.00	364.26	620.88	-1.89	0.29	0.44	2.02	23.73
14	Pangduo	5015	Brahmaputra	16459.00	348.31	544.59	-1.53	0.27	0.33	1.66	23.33
15	Tangjia	4982	Brahmaputra	20143.00	350.61	555.17	-1.89	0.27	0.34	1.39	21.83
16	Gongbujiangda	4927	Brahmaputra	6417.00	586.96	692.06	-4.24	0.27	0.36	4.12	25.99
17	Nuxia	2910	Brahmaputra	191235.00	307.38	401.35	-0.73	0.22	0.25	1.90	13.50
18	Yangcun	3600	Brahmaputra	152701.00	163.25	349.91	-0.87	0.19	0.18	1.28	10.52

Table 2: Overview of multi-source datasets applied in this study

Data category	Data source	Spatial resolution	Temporal resolution	Available period used	Reference
Runoff (Q)	Observed, National Hydrology Almanac of China	—	Daily	1982-2011	—
	VIC_IGSNRR simulated	0.25°	Daily	1982-2011	Zhang et al. (2014)
Precipitation (P)	Observed, CMA	0.5 °	Monthly	1982-2011	—
	TRMM 3B43 V7	0.25°	Monthly	2000-2011	Huffman et al. (2012)
	IGSNRR forcing	0.25°	Daily	1982-2011	Zhang et al. (2014)
Temperature (Temp.)	Observed, CMA	0.5 °	Monthly	2000-2011	—
Terrestrial storage change	GRACE-CSR	Approx.300-400 km	Monthly	2002-2011	Tapley et al. (2004)
(ΔS)	GRACE-GFZ	Approx.300-400 km	Monthly	2002-2011	Tapley et al. (2004)
	GRACE-JPL	Approx.300-400 km	Monthly	2002-2011	Tapley et al. (2004)
Potential evaporation (PET)	CRU	0.5 °	Monthly	1982-2011	Harris et al. (2013)
Actual evaporation (ET)	MTE_E	0.5 °	Monthly	1982-2011	Jung et al. (2010)
	VIC_E	0.25°	Daily	1982-2011	Zhang et al. (2014)
	GLEAM_E	0.25°	Daily	1982-2011	Miralles et al. (2011)
	PML_E	0.5 °	Monthly	1982-2011	Zhang Y et al. (2016)
	Zhang_E	8 km	Monthly	1983-2006	Zhang et al. (2010)
	GNoah_E	1.0 °	3 hourly	1982-2011	Rui (2011)
NDVI	GIMMS NDVI dataset	8 km	15 daily	1982-2011	Tucker et al. (2005)
LAI	GLASS LAI Product	0.05°	8 daily	1982-2011	Liang and Xiao (2012)
Snow Cover	TP Snow composite Products	500 m	Daily	2005-2013	Zhang et al. (2012)
SWE	VIC_IGSNRR simulated	0.25°	Daily	1982-2011	Zhang et al. (2014)
	GlobSnow-2 Product	25 km	Daily	1982-2011	Takala et al. (2011)

Table 3: Contribution of glacier-melt to discharge in eighteen basins ("—" shows no glacier influences, "—*" shows the percentage is empirically estimated through the relation between lacier area ratio and glacier melt for basins in which the glacier melt contribution has been reported in ~~existing studies~~ the literatures)

Basin	Contributions of glacier-melt to discharge (%)	Reference
Kulukelangan	62.73	Mansur and Ajnisa (2005)
Tongguziluoke	64.90	Liu J et al. (2016)
Numaitilangan	71	Chen (1988)
Zelingou	—	—
Gadatan	—	—
Xining	—	—
Tongren	—	—
Tainaihai	0.80	Zhang et al. (2013)
Huangheyan	—	—
Jimai	—	—
Yajiang	1.40	—*
Zhimenda	6.50	Zhang et al. (2013)
Jiaoyuqiao	4.80	Zhang et al. (2013)
Nuxia	11.60	Zhang et al. (2013)
Pangduo	10.13	—*
Tangjia	8.49	—*
Gongbujiangda	25.15	—*
Yangcun	7.81	—*

Table 4: Nonparametric trends for different ET estimates during the period 1982-2006 detected by modified Mann-Kendall test, the bold number showed the detected trend is statistically significant at the 0.05 level

Basin	ET_{wb}	GLEAM_E	VIC_E	Zhang_E	PML_E	MET_E	GNoah_E
Kulukelangan	**-0.09**	0.09	**0.18**	_	0.03	-0.01	0.07
Tongguziluoke	-0.02	0.10	**0.13**	_	0.03	**-0.08**	0.19
Numaitilangan	0.04	**0.10**	0.14	_	0.14	**-0.10**	0.22
Zelingou	**0.13**	**0.23**	0.11	**0.09**	0.04	**0.06**	0.02
Gadatan	-0.09	0.25	0.070	-0.10	-0.01	**0.06**	-0.07
Xining	-0.06	**0.54**	0.01	-0.08	0.01	0.02	-0.06
Tongren	-0.06	**0.34**	-0.15	**-0.17**	0.07	0.02	0.13
Tainaihai	0.06	**0.28**	-0.03	**-0.11**	0.04	**0.05**	0.04
Huangheyan	0.08	**0.19**	-0.01	**-0.10**	**0.08**	**0.05**	**0.10**
Jimai	-0.07	**0.23**	-0.01	-0.08	0.03	**0.05**	0.10
Yajiang	0.17	**0.26**	**0.06**	**-0.21**	-0.01	0.03	-0.02
Zhimenda	0.11	**0.28**	0.10	0.01	0.07	**0.04**	0.07
Jiaoyuqiao	**0.18**	**0.28**	0.10	**-0.11**	0.05	**0.05**	0.07
Nuxia	**-0.09**	**0.25**	0.09	**-0.10**	**0.12**	**0.04**	0.10
Pangduo	0.05	**0.28**	**0.17**	**-0.07**	0.07	**0.07**	**0.11**
Tangjia	0.09	**0.26**	**0.17**	**-0.09**	**0.20**	**0.06**	**0.12**
Gongbujiangda	-0.26	0.12	0.13	**-0.16**	**0.19**	0.01	**0.15**
Yangcun	0.03	**0.28**	0.08	**-0.06**	0.10	0.04	0.09

Figure captions:

Figure1. Map of river basins and hydrological gauging stations (green dots) over the Tibetan Plateau (TP) used in this study. The grey shading shows the topography of TP in meters above the sea level and the blue shading exhibits the glaciers distribution in TP extracted from the Second Glacier Inventory Dataset of China.

Figure 2. Comparison of VIC_IGSNRR simulated and observed monthly runoff for Tangnaihai and Panduo stations (a and b) as well as (c) basin-averaged monthly TRMM, CMA gridded and IGSNRR forcing precipitations for the smallest basin (Tongren station) over the period 1982-2011. (d) shows the comparison of TRMM (blue) and IGSNRR forcing (red) precipitations against CMA gridded precipitation for 18 river basins over TP during the period 2000-2011.

Figure 3. Comparison of different ET products against the calculated ET through the water balance method (ET_{wb}) for 18 TP basins. The boxplot of annual estimates of different ET products for 18 TP basins are shown in (a) while the correlation coefficients and root-mean-square-errors (RMSEs, mm/month) for each ET product relatively to ET_{wb} are exhibited in (b).

Figure 4. General water and energy status (a. the perspective of Budyko framework) and their relationships with glacier (b) and vegetation (c and d) for eighteen TP river basins (1983-2006). The ET used in this figure is calculated from the bias-corrected water balance method.

Figure 5. Seasonal cycles (1982-2011) of water budget components in westerlies-dominated (column 1), East Asian monsoon-dominated (columns 2-4) and Indian monsoon-dominated (columns 5-6) TP basins.

Figure 6. Seasonal cycles (1982-2011) of air temperature and vegetation parameters in westerlies-dominated (column 1), East Asian monsoon-dominated (columns 2-4) and Indian monsoon-dominated (columns 5-6) TP basins.

Figure 7. Seasonal cycles (1982-2011) of snow cover and snow water equivalent (SWE) in westerlies-dominated (column 1), East Asian monsoon-dominated (columns 2-4) and Indian monsoon-dominated (columns 5-6) TP basins. The snow cover was

extracted from cloud free snow composite product during the period 2005-2013. It should also be noted that the GlobSnow data are not available for some basins.

Figure 8. Sen's slopes of water budget components and vegetation parameters in westerlies-dominated TP basins during the period of 1982-2011. The double red stars showed that the trend was statistically significant at the 0.05 level.

Figure 9. Linear and non-parametric trends of westerly, Indian monsoon and East Asian summer monsoon during the period 1982-2011 revealed prospectively by the Asian Zonal Circulation Index, Indian Ocean Dipole Mode Index and East Asian Summer Monsoon Index.

Figure 10. Similar to Figure 8 but for East Asian monsoon-dominated TP basins. It should be noted that the GlobSnow data are not available for some basins. The double red stars showed that the trend was statistically significant at the 0.05 level.

Figure 11. Similar to Figure 8 but for Indian monsoon-dominated TP basins. It should be noted that the GlobSnow data are not available for some basins.The double red stars showed that the trend was statistically significant at the 0.05 level.

Figure 1. Map of river basins and hydrological gauging stations (green dots) over the Tibetan Plateau (TP) used in this study. The grey shading shows the topography of TP in meters above the sea level and the blue shading exhibits the glaciers distribution in TP extracted from the Second Glacier Inventory Dataset of China.

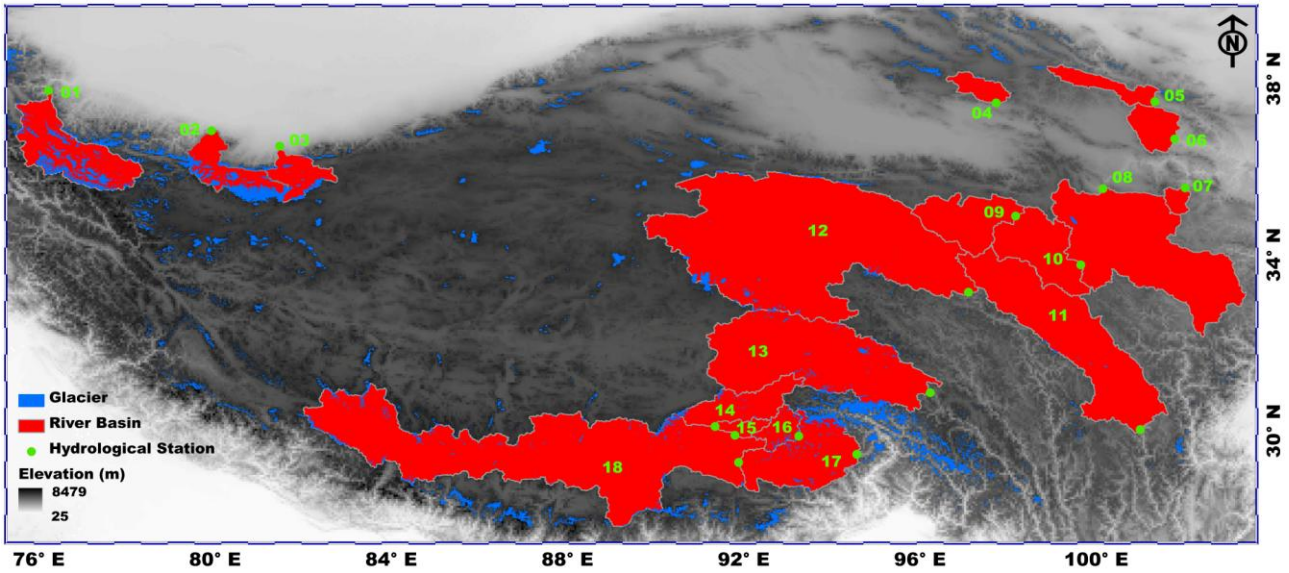

Figure 2. Comparison of VIC_IGSNRR simulated and observed monthly runoff for Tangnaihai and Panduo stations (a and b) as well as (c) basin-averaged monthly TRMM, CMA gridded and IGSNRR forcing precipitations for the smallest basin (Tongren station) over the period 1982-2011. (d) shows the comparison of TRMM (blue) and IGSNRR forcing (red) precipitations against CMA gridded precipitation for 18 river basins over TP during the period 2000-2011.

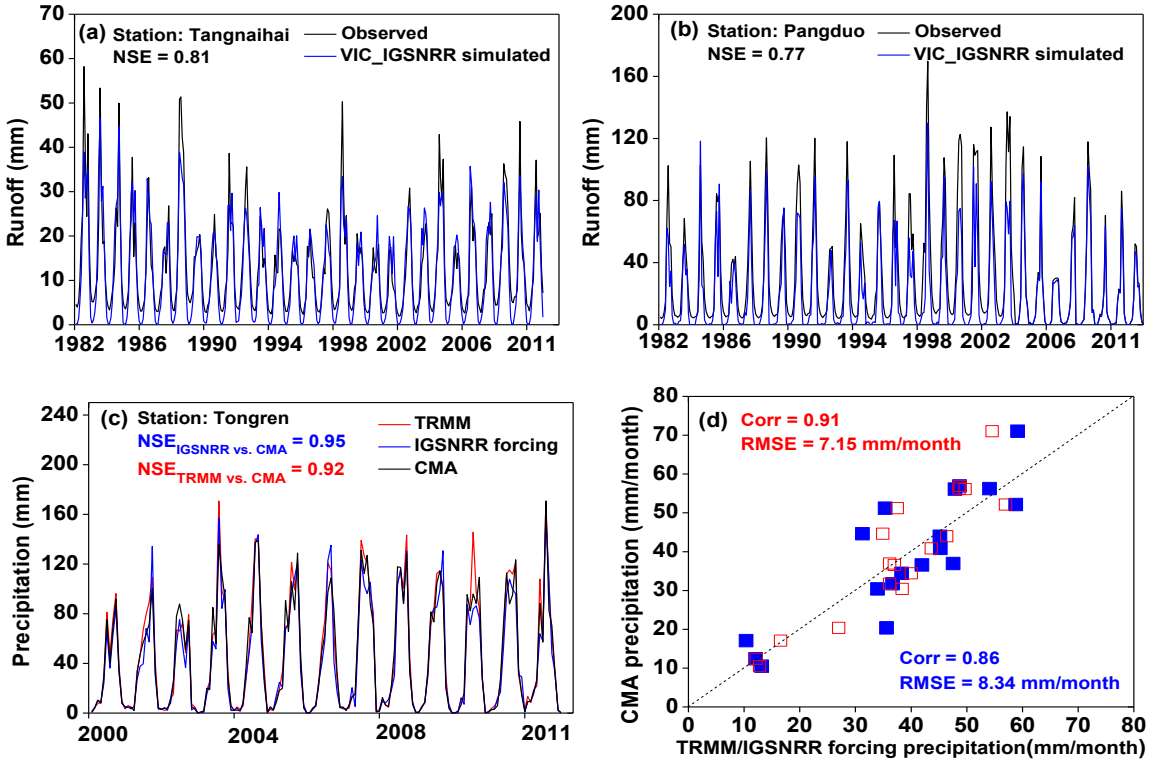

Figure 3. Comparison of different ET products against the calculated ET through the water balance (ET_{wb}) for 18 river basins over the Tibetan Plateau. The boxplot of annual estimates of different ET products for 18 TP basins are shown in (a) while the correlation coefficients and root-mean-square-errors (RMSEs, mm/month) for each ET product relatively to ET_{wb} are exhibited in (b).

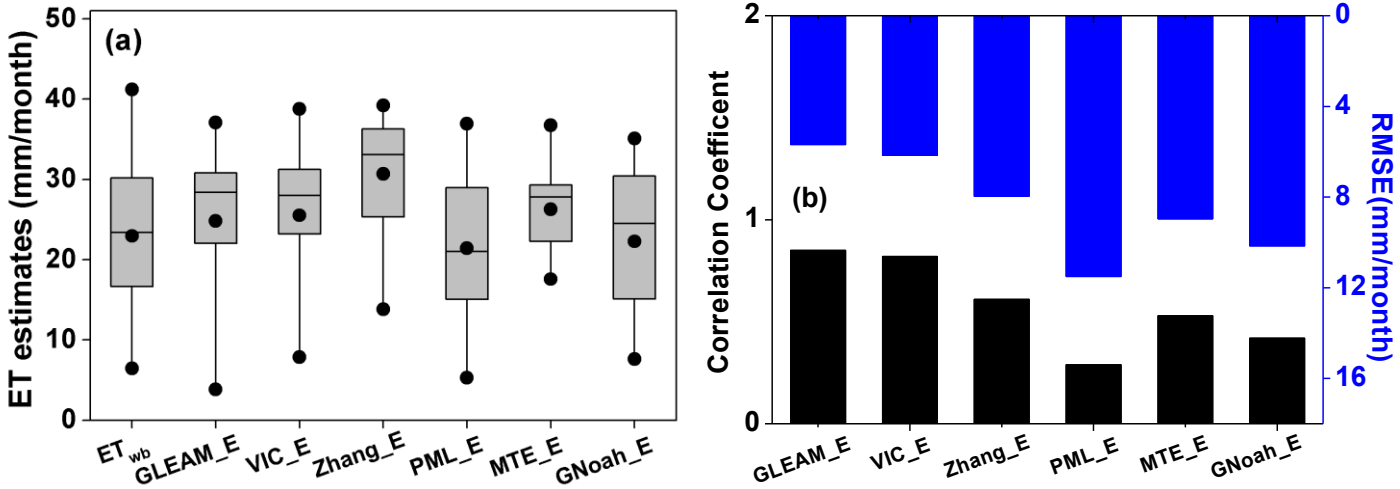

Figure 4. General water and energy status (a. the perspective of Budyko framework) and their relationships with glacier (b) and vegetation (c and d) for eighteen TP river basins (1983-2006). The ET used in this figure is calculated from the bias-corrected water balance method.

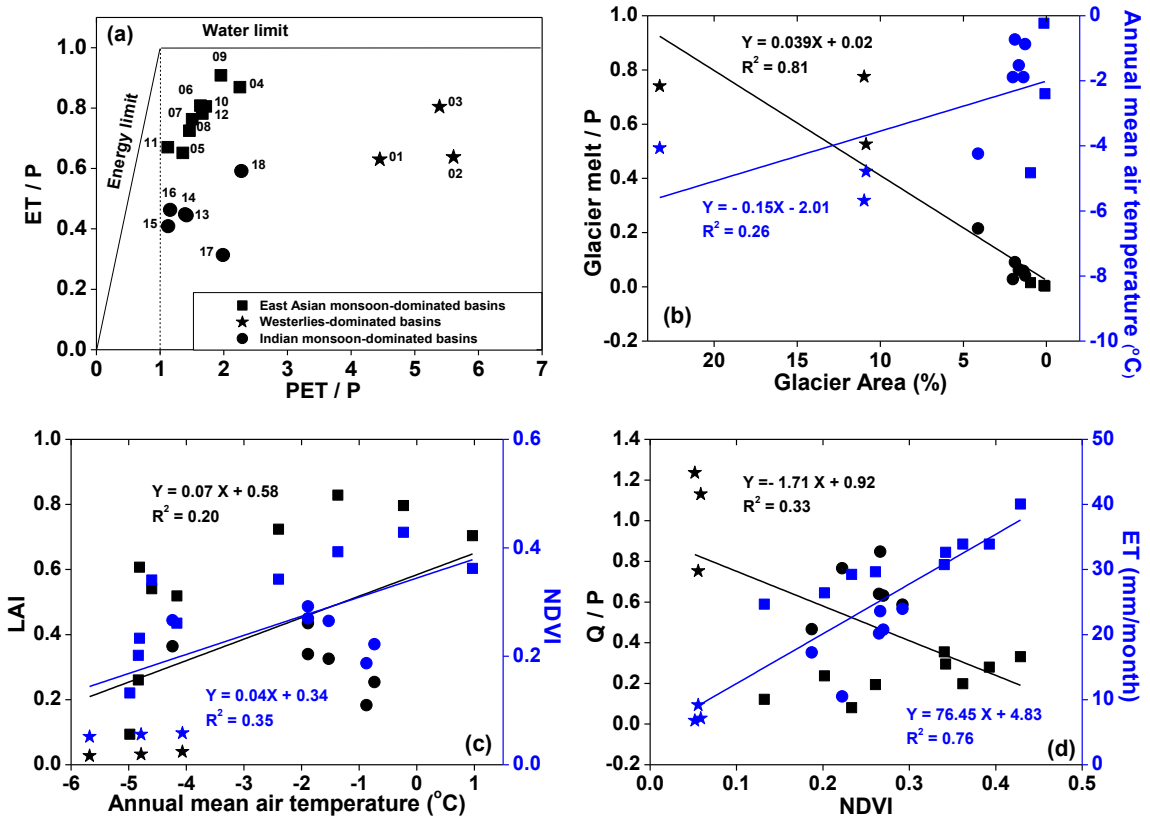

Figure 5. Seasonal cycles (1982-2011) of water budget components in westerlies-dominated (column 1), East Asian monsoon-dominated (columns 2-4) and Indian monsoon-dominated (columns 5-6) TP basins.

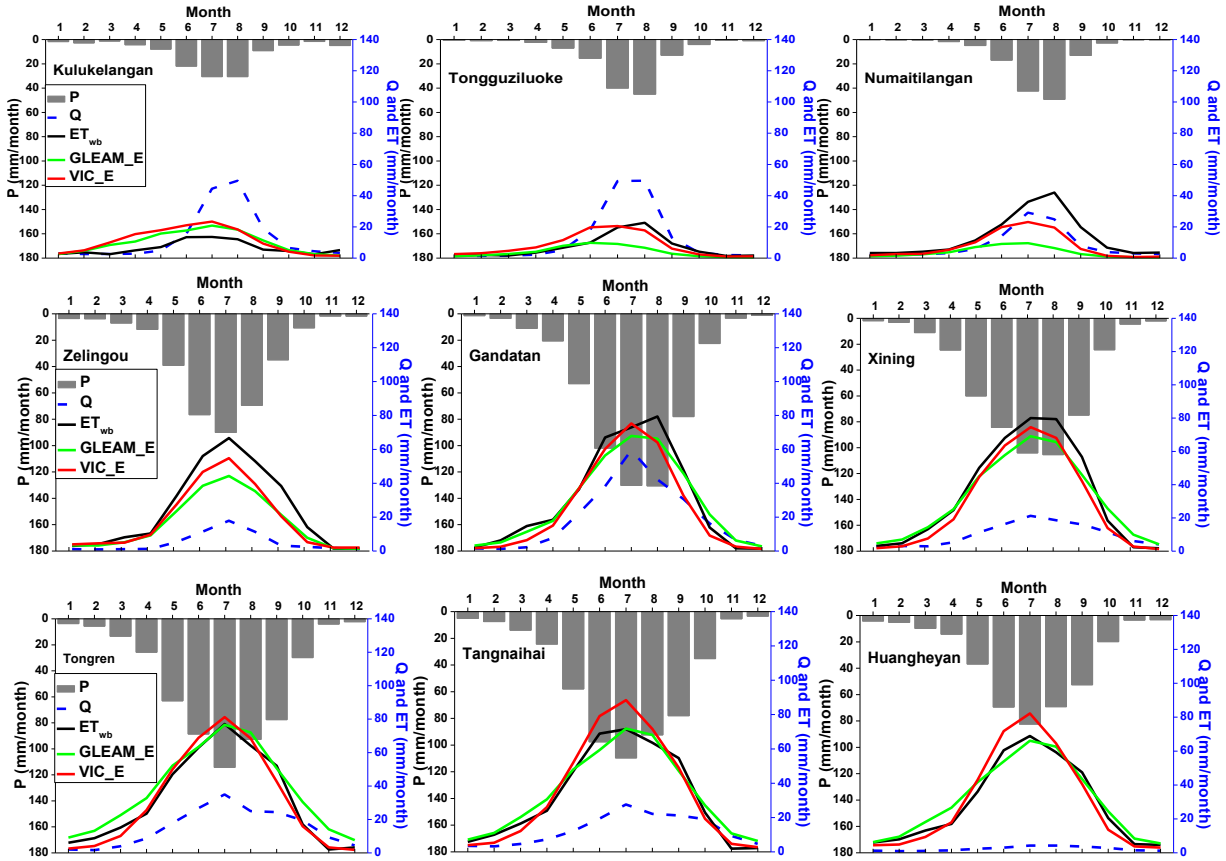

Figure 5: (continued)

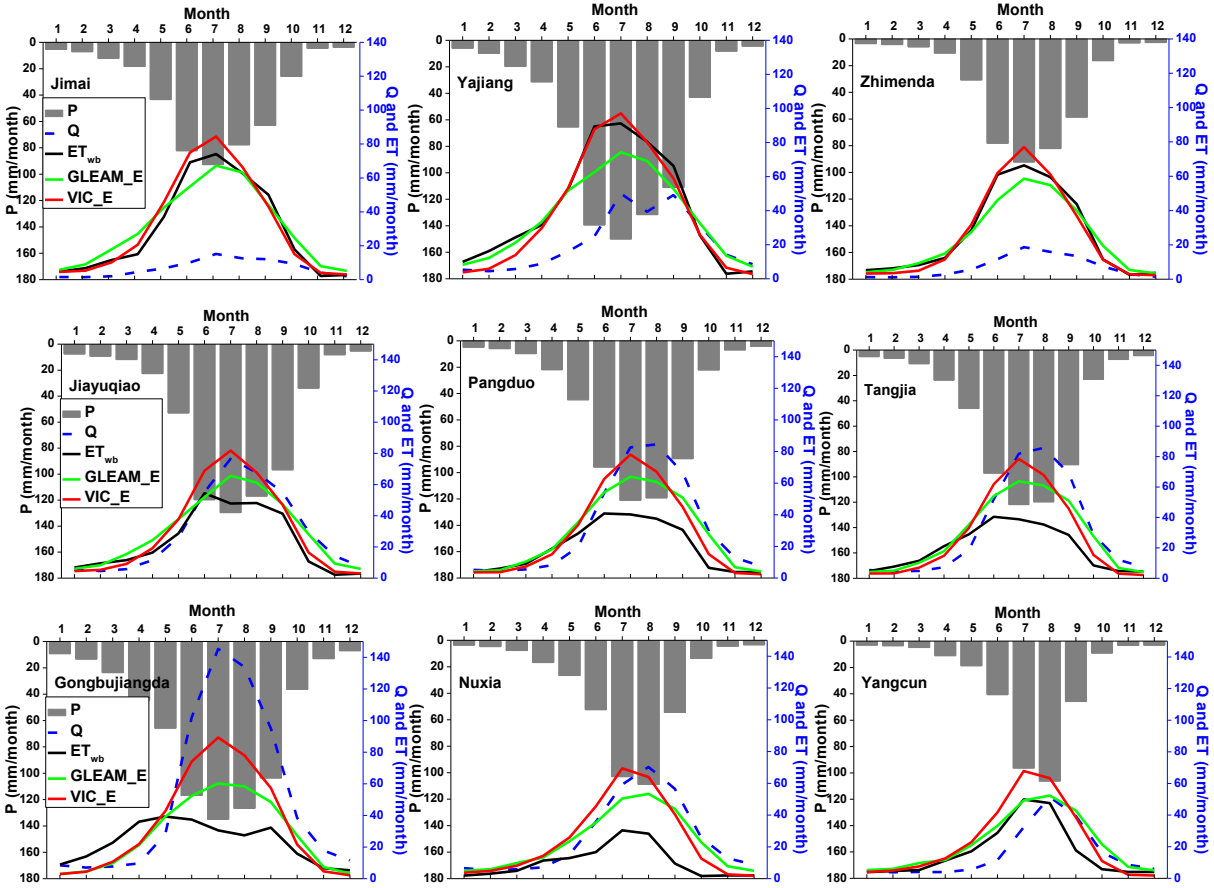

Figure 6. Seasonal cycles (1982-2011) of air temperature and vegetation parameters in westerlies-dominated (column 1), East Asian monsoon-dominated (columns 2-4) and Indian monsoon-dominated (columns 5-6) TP basins.

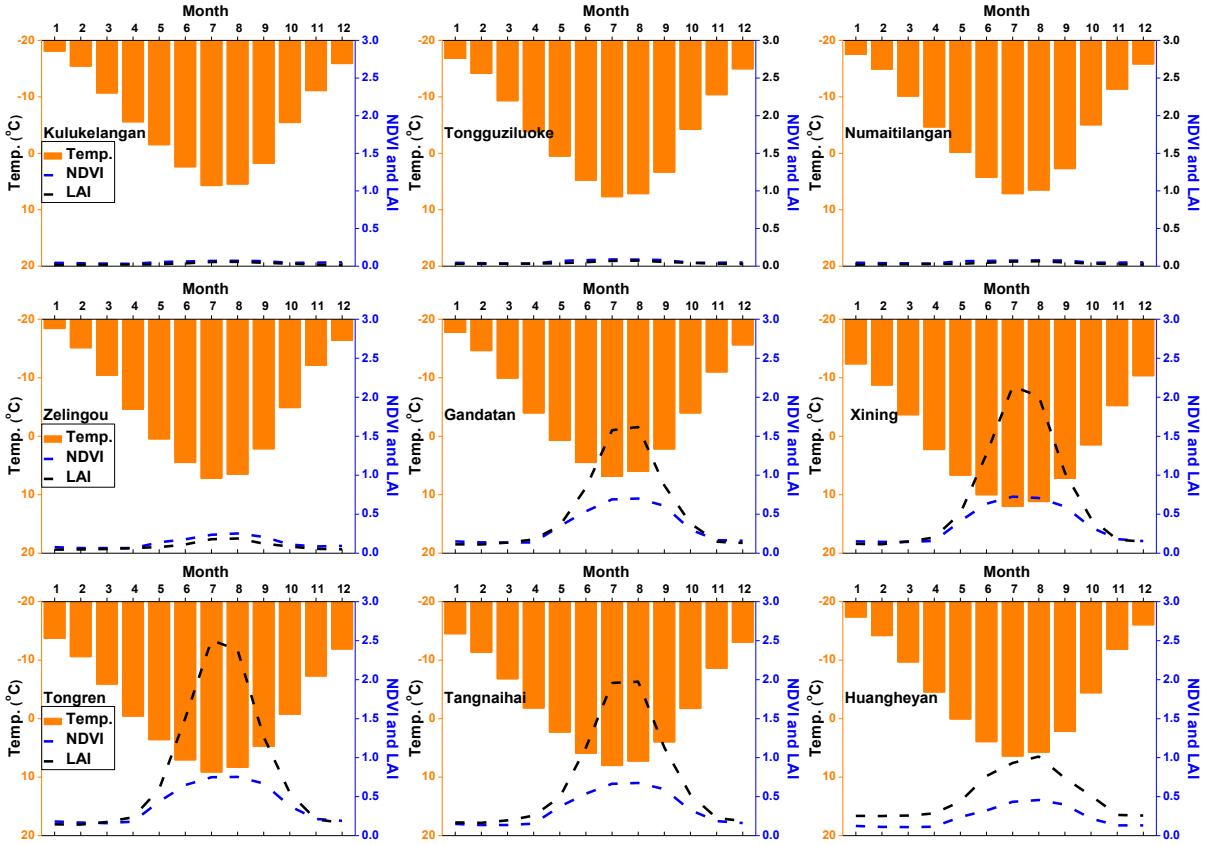

Figure 6: (continued)

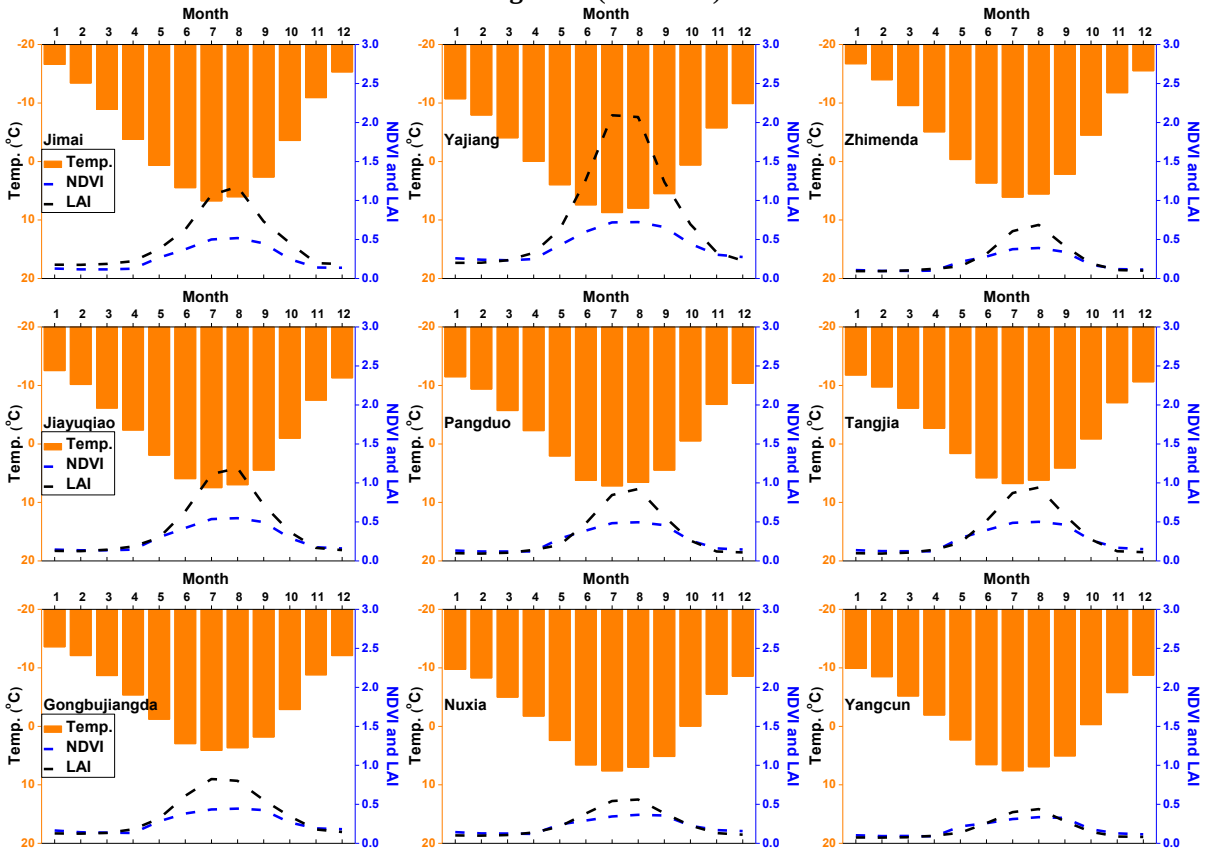

940 **Figure 7**. Seasonal cycles (1982-2011) of snow cover and snow water equivalent (SWE) in westerlies-dominated (column 1), East Asian monsoon- dominated
941 (columns 2-4) and Indian monsoon-dominated (columns 5-6) TP basins. The snow cover was extracted from cloud free snow composite product during the period
942 2005-2013. It should also be noted that the GlobSnow data are not available for some basins.
943

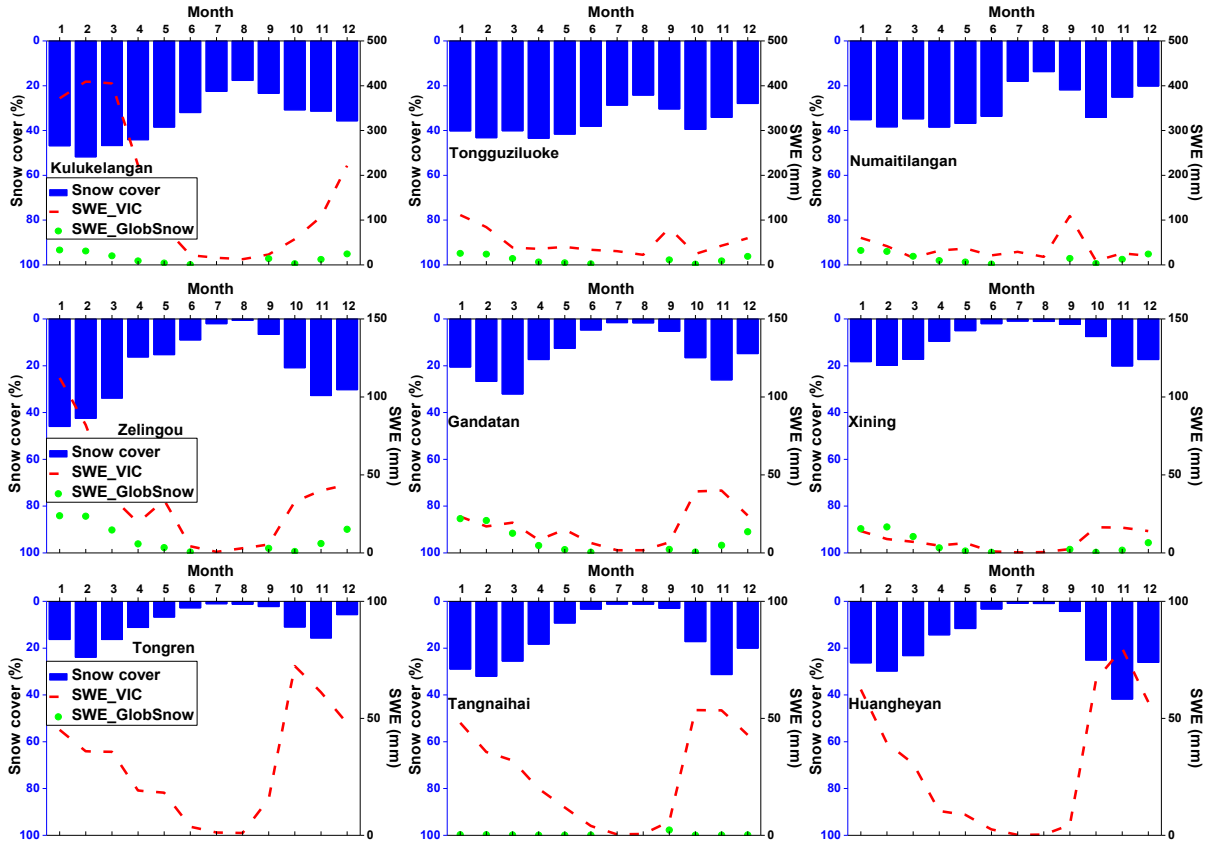
Month
Snow cover (%)
SWE (mm)
Kulukelangan
Tongguziluoke
Numaitilangan
Zelingou
Gandatan
Xining
Tongren
Tangnaihai
Huangheyan
Snow cover
SWE_VIC
SWE_GlobSnow

Figure 7: (continued)

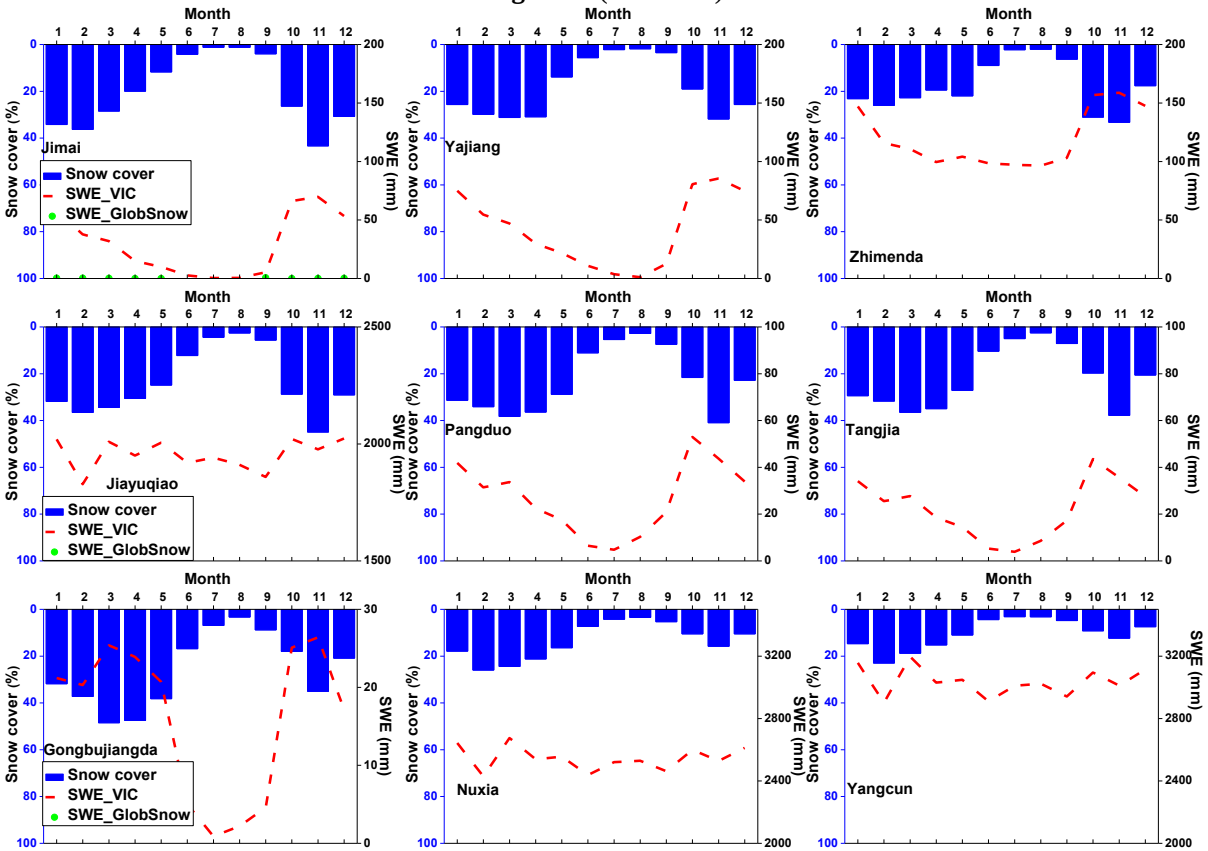

Figure 8. Sen's slopes of water budget components and vegetation parameters in westerlies-dominated TP basins during the period of 1982-2011. The double red stars showed that the trend was statistically significant at the 0.05 level.

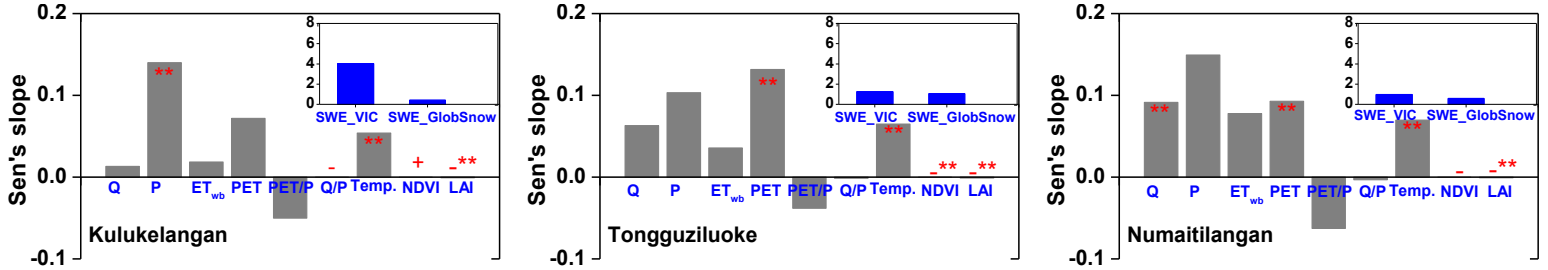

Figure 9. Linear and non-parametric trends of westerly, Indian monsoon and East Asian summer monsoon during the period 1982-2011 revealed prospectively by the Asian Zonal Circulation Index, Indian Ocean Dipole Mode Index and East Asian Summer Monsoon Index.

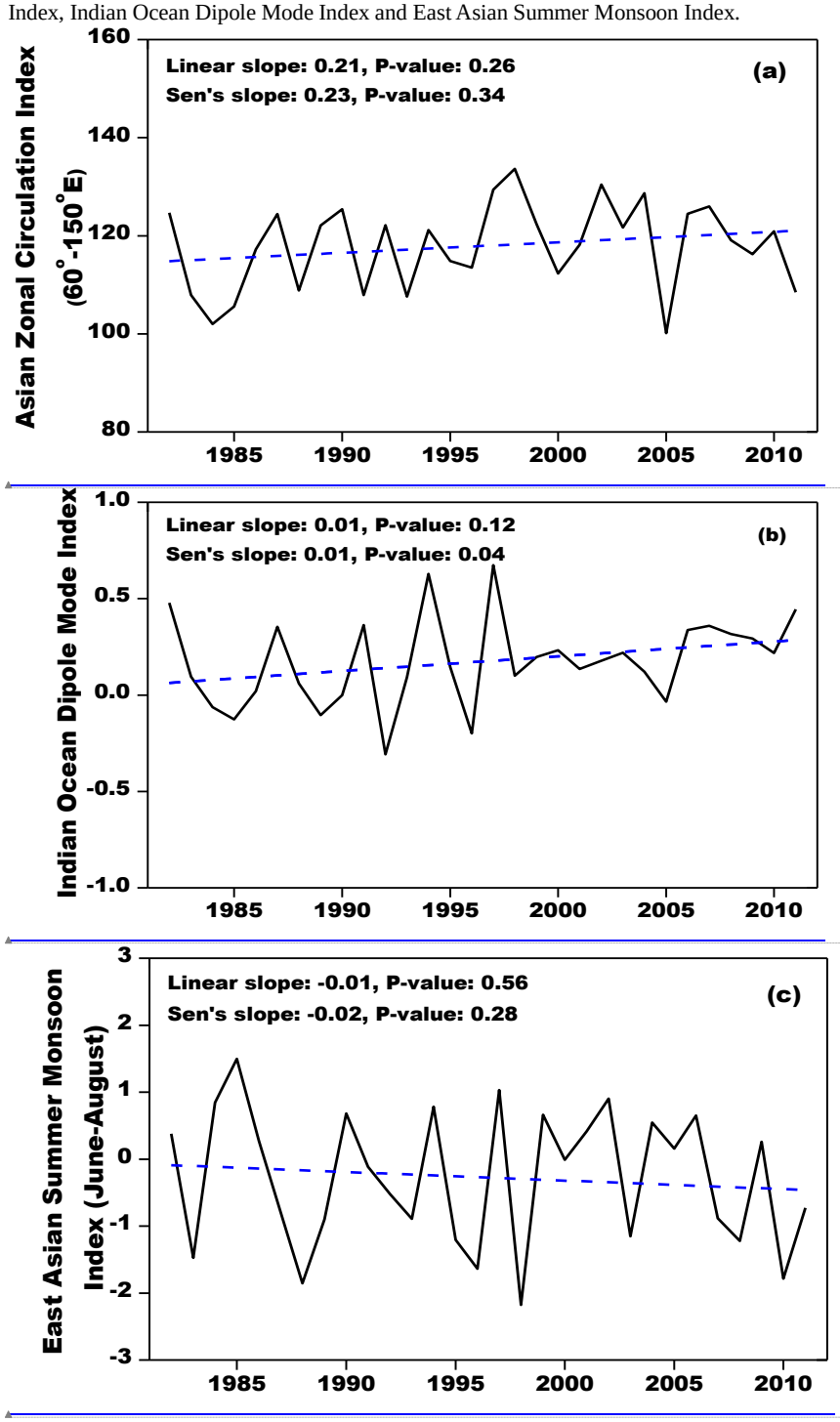

域代码已更改

域代码已更改

带格式的：左

域代码已更改

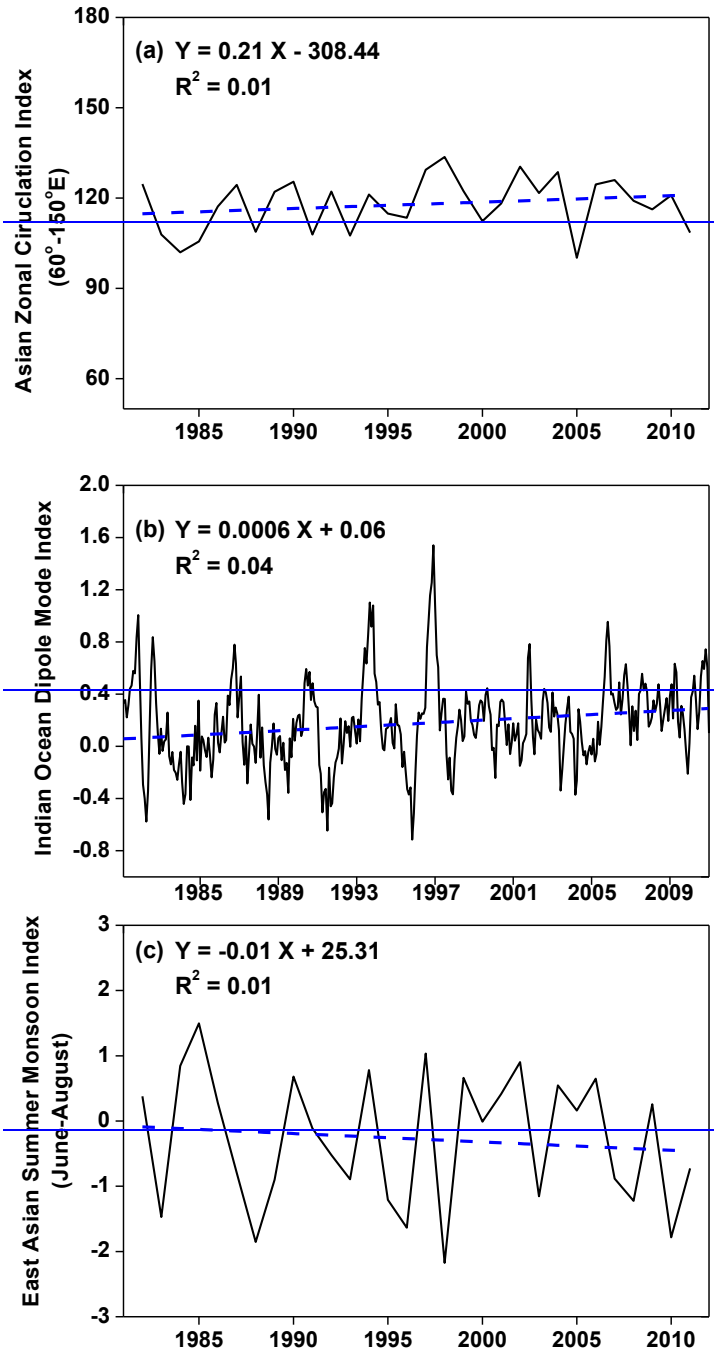

964

965

966

967

968

带格式的：两端对齐

Figure 10. Similar to Figure 8 but for East Asian monsoon-dominated TP basins. It should be noted that the GlobSnow data are not available for some basins. The double red stars showed that the trend was statistically significant at the 0.05 level.

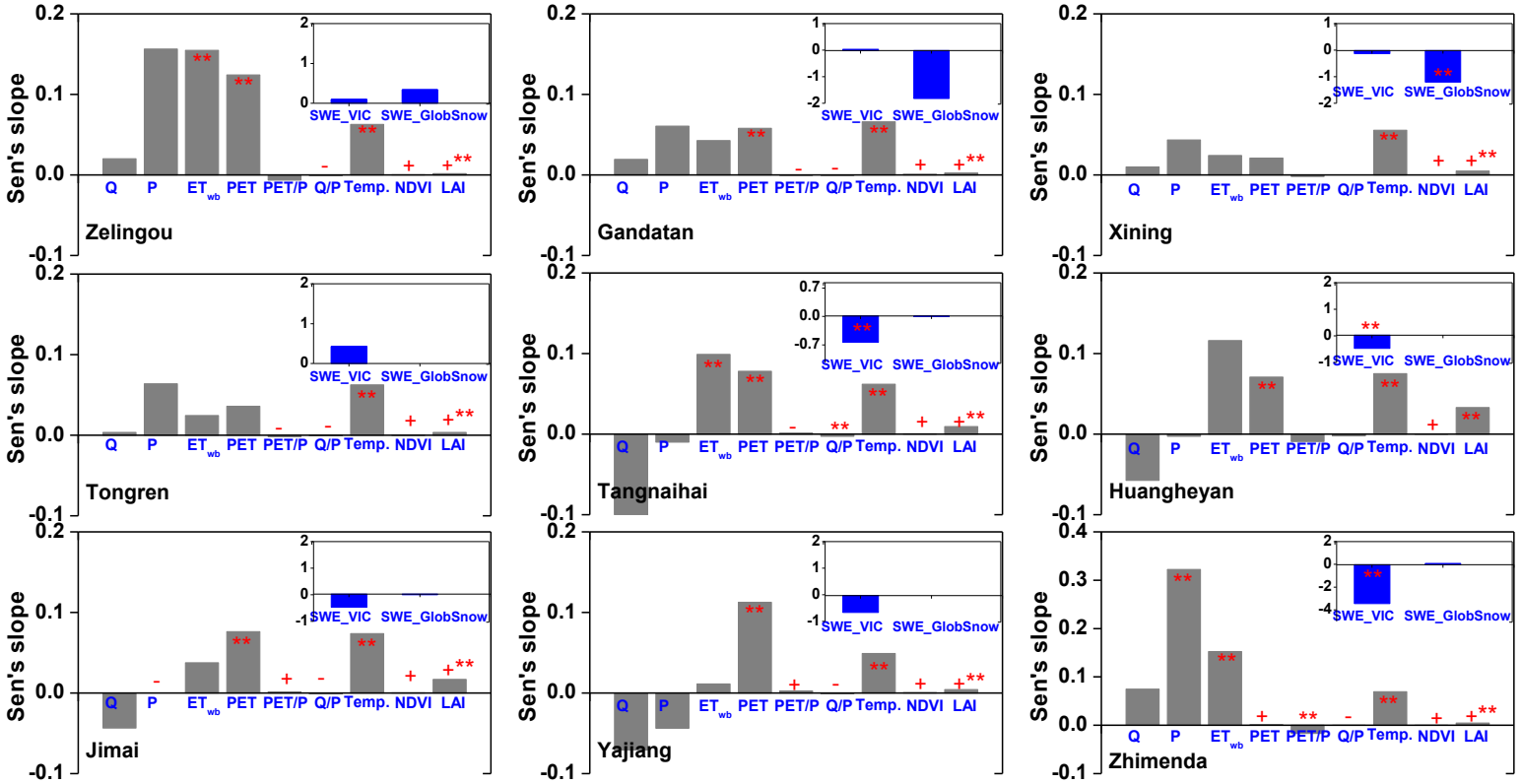

Figure 11. Similar to Figure 8 but for Indian monsoon-dominated TP basins. It should be noted that the GlobSnow data are not available for some basins. The double red stars showed that the trend was statistically significant at the 0.05 level.